Le manteau terrestre
&
magmas derivés

5.2

16h CM; 13h TP + visite Labo CRPG

pierre.bouilhol@univ-lorraine.fr

5.2 Magmas & Manteau

GENERALITES

- Manteau (2H) → TP Manteau 3H
- Basaltes (2H)

Pétrogenèses des liquides / Géodynamique

- MORB (4H) → TP cumulats 2H
- Subduction (4H) → TP volc. Sub. 2H / TP Rapport 3H
- Point chaud (4H) → TP Serie Alc. 3H

3H visite CRPG / C. Cartier

BUT

- Connaitre les bases de formation et d'évolution des magmas (primaire) dans leur contexte géodynamique

→Module très dense / Etre à la hauteur du défi…

…Contrôle inopiné…?

CC

- OFFICIELLEMENT:

Contrôle Final de 2H. Une partie cours / une partie dissert.

→TP: un petit Contrôle conti. / niveau pétrographique

→TP: un rapport sur une étude de cas

Plan

- Le manteau: définition
- Le Géotherme
- Minéralogie du Manteau Inf., transition de phases
- Mineralogie du Manteau Sup., relation Manteau / Basaltes
- Geochimie du manteau
- Transformations

Le manteau terrestre

- Observation directes

→Affleurement (orogénique-ophiolite-abyssal) / Xénolites

- Observations indirectes

→Géophysiques

- Observations Expérimentales

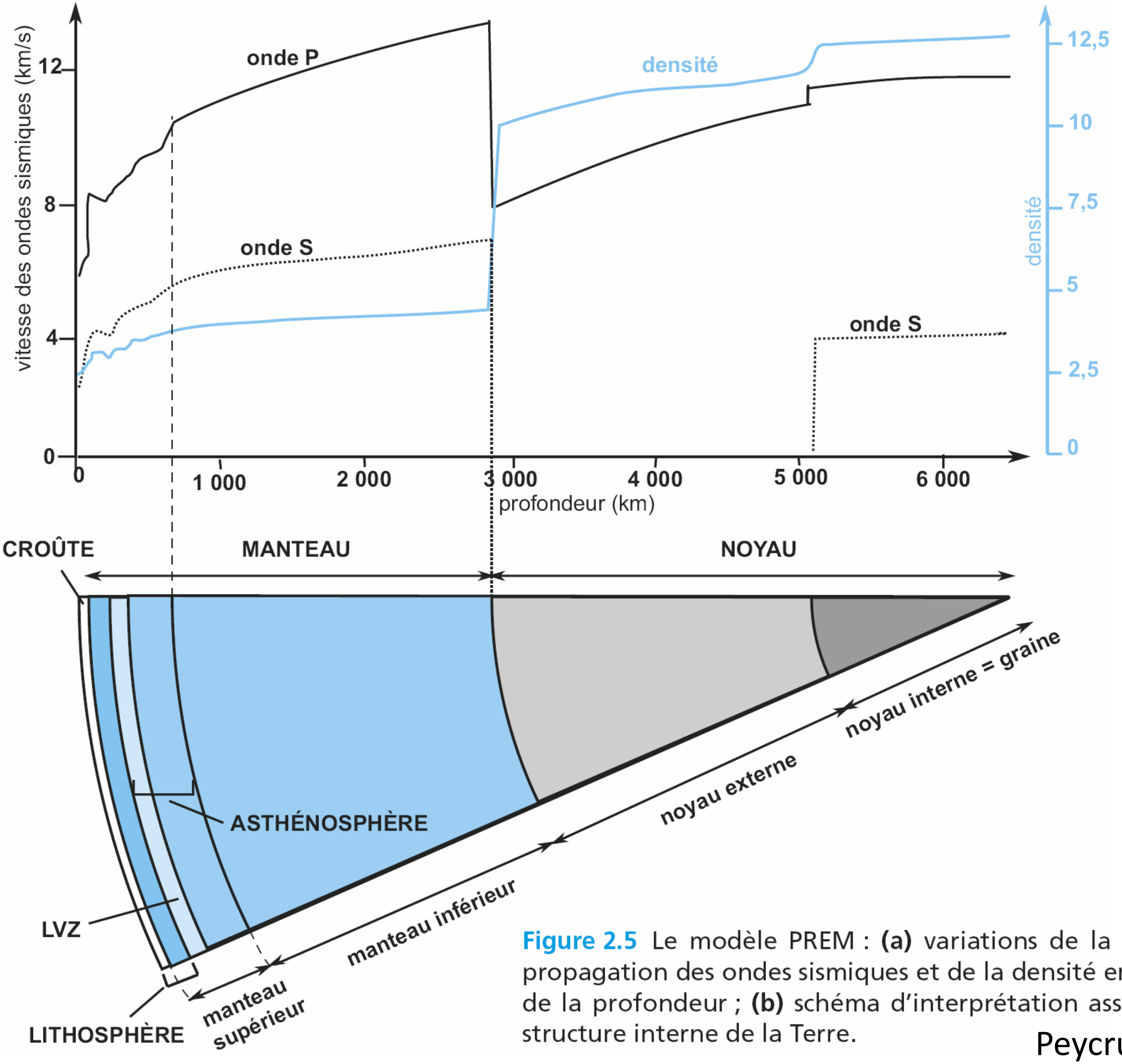

Figure 2.5 Le modèle PREM : **(a)** variations de la vitesse de propagation des ondes sismiques et de la densité en fonction de la profondeur ; **(b)** schéma d'interprétation associé de la structure interne de la Terre.

Peycru (Geol tt-en-1)

Lithosphere

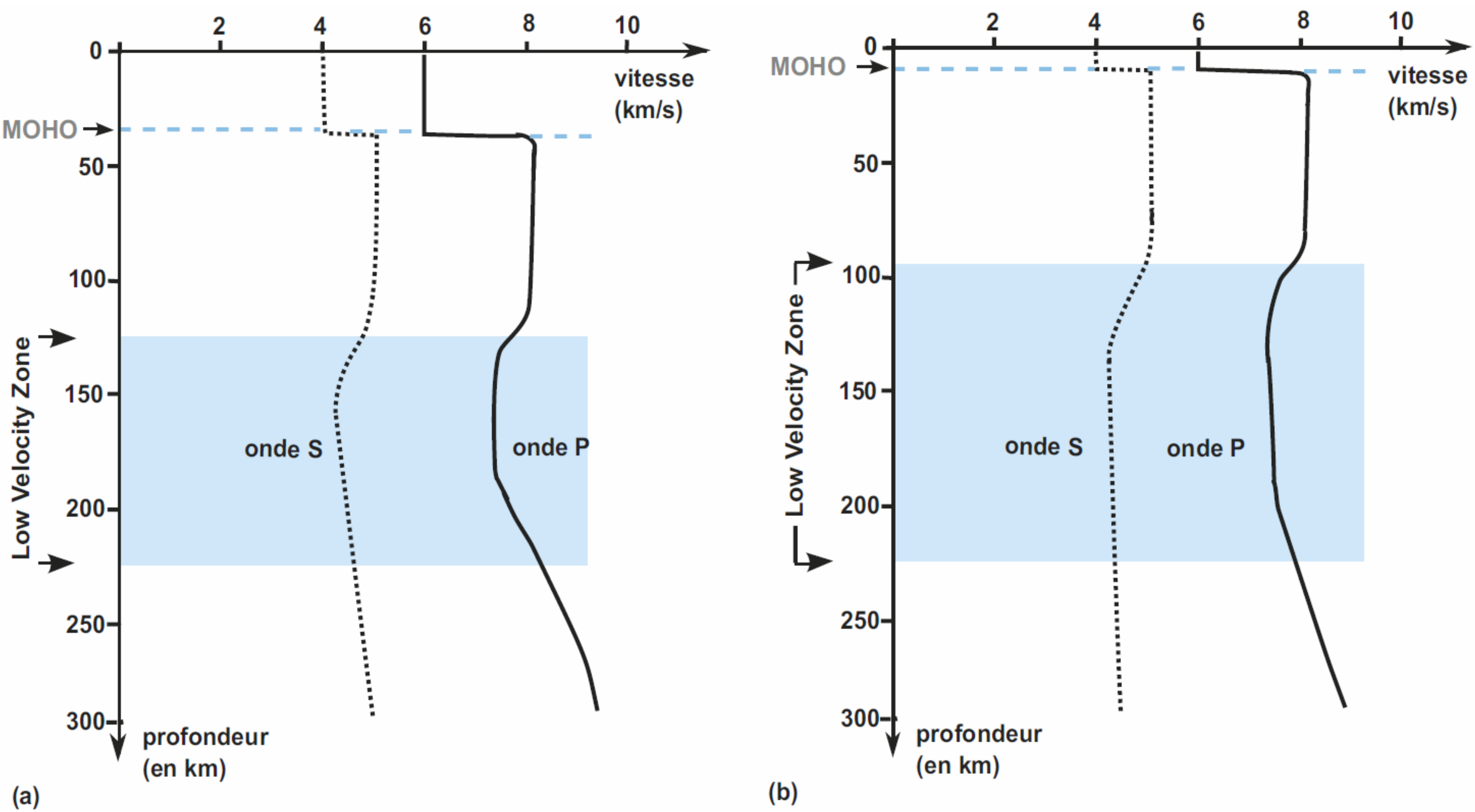

Figure 2.4 Variation de la vitesse de propagation des ondes P et S sous les continents **(a)** et sous les océans **(b)**.

Peycru (Geol tt-en-1)

Taille

- Volume = 82 % du volume de la Terre
- Masse = 65 % de la masse de la Terre
- S'étend de la base de la croûte (6-70 km) jusqu'à l'interface avec le noyau (2900 km)

Terre:	5.97 10^{24} kg
Noyau interne ou graine:	9.84 10^{22} kg
Noyau externe:	1.84 10^{24} kg
Manteau:	4.00 10^{24} kg
Manteau supérieur	2.94 10^{24} kg
Manteau inférieur	1.06 10^{24} kg
Croûtes océaniques + continentales:	2.97 10^{22} kg

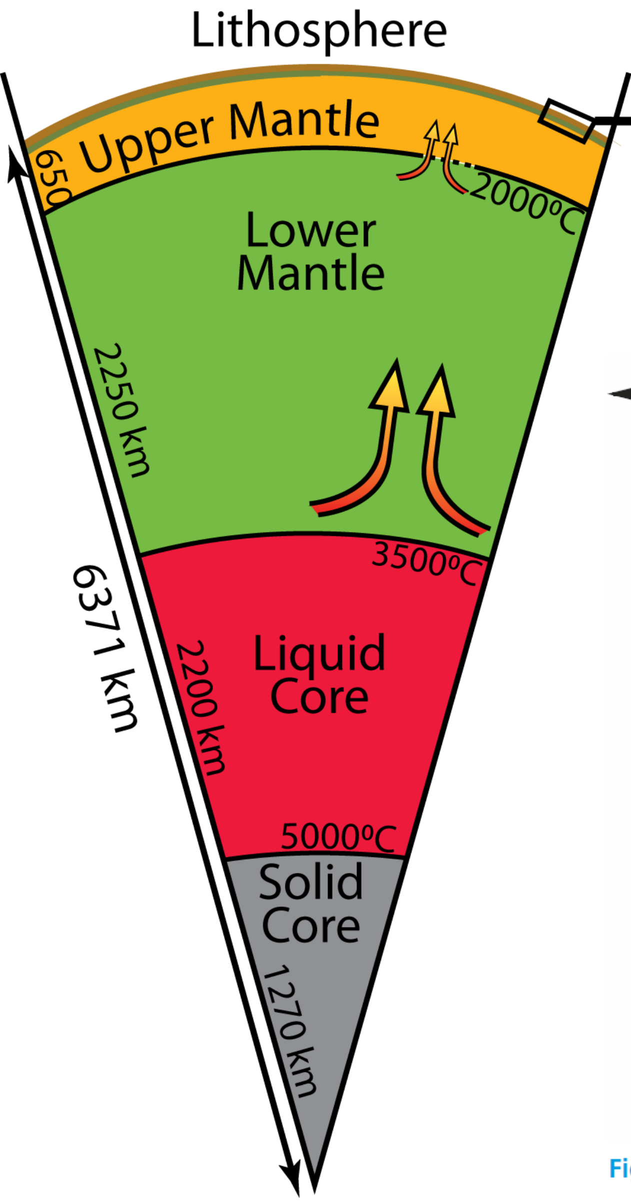

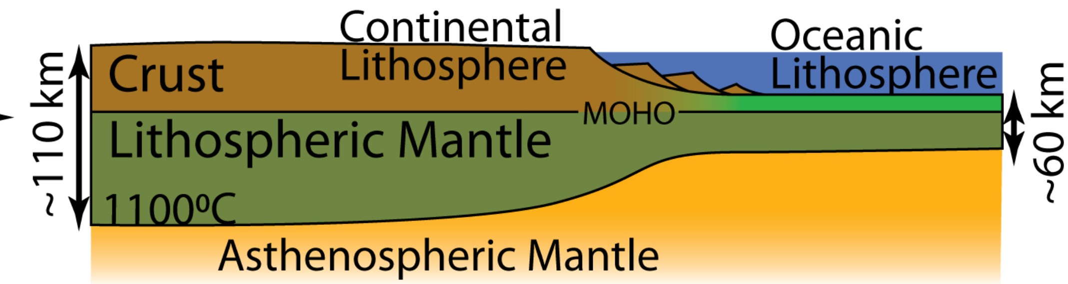

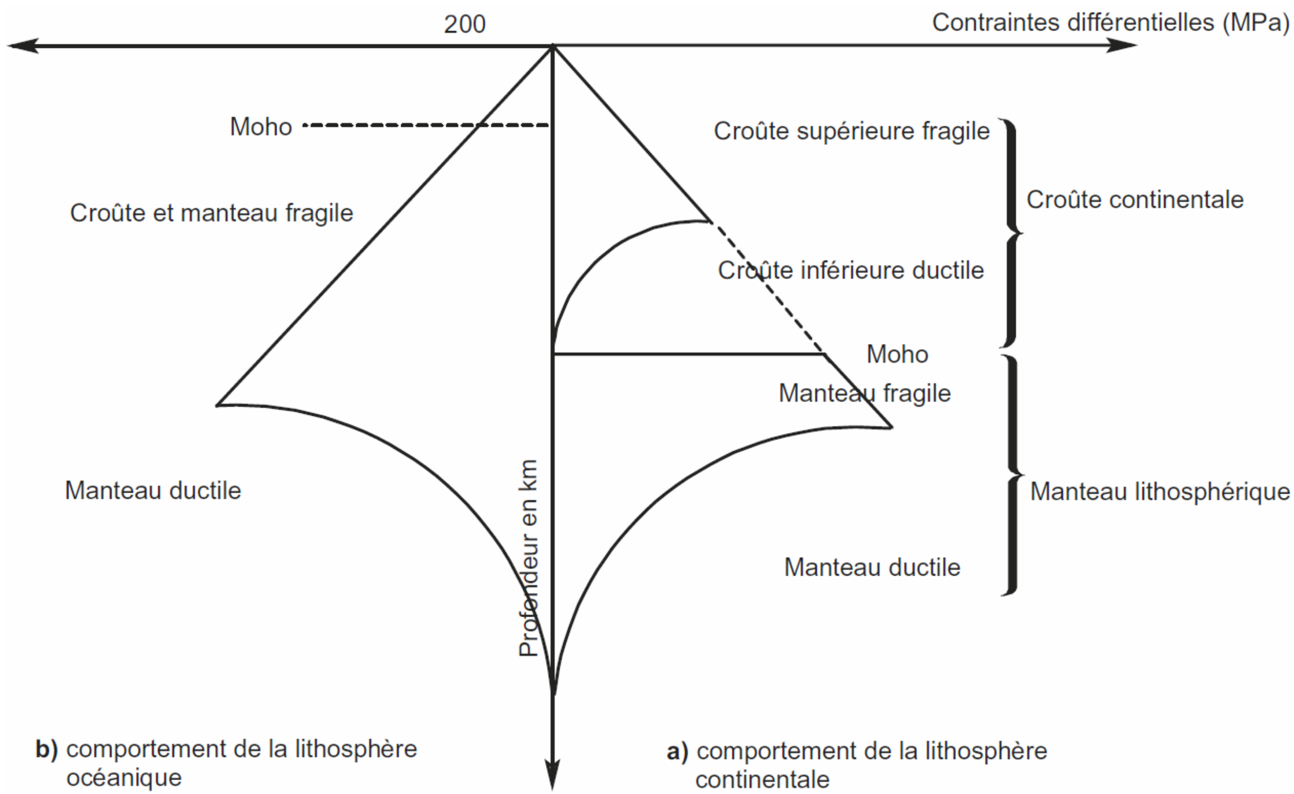

Figure 10.30 Profils rhéologiques de la lithosphère continentale **(a)** et de la lithosphère océanique **(b)**.

Fluage, convection, compare a lithosphere ou resistance mecanique ++++ → implication tectonique et magma percolation

Deformation lithospherique vs asthenopherique.

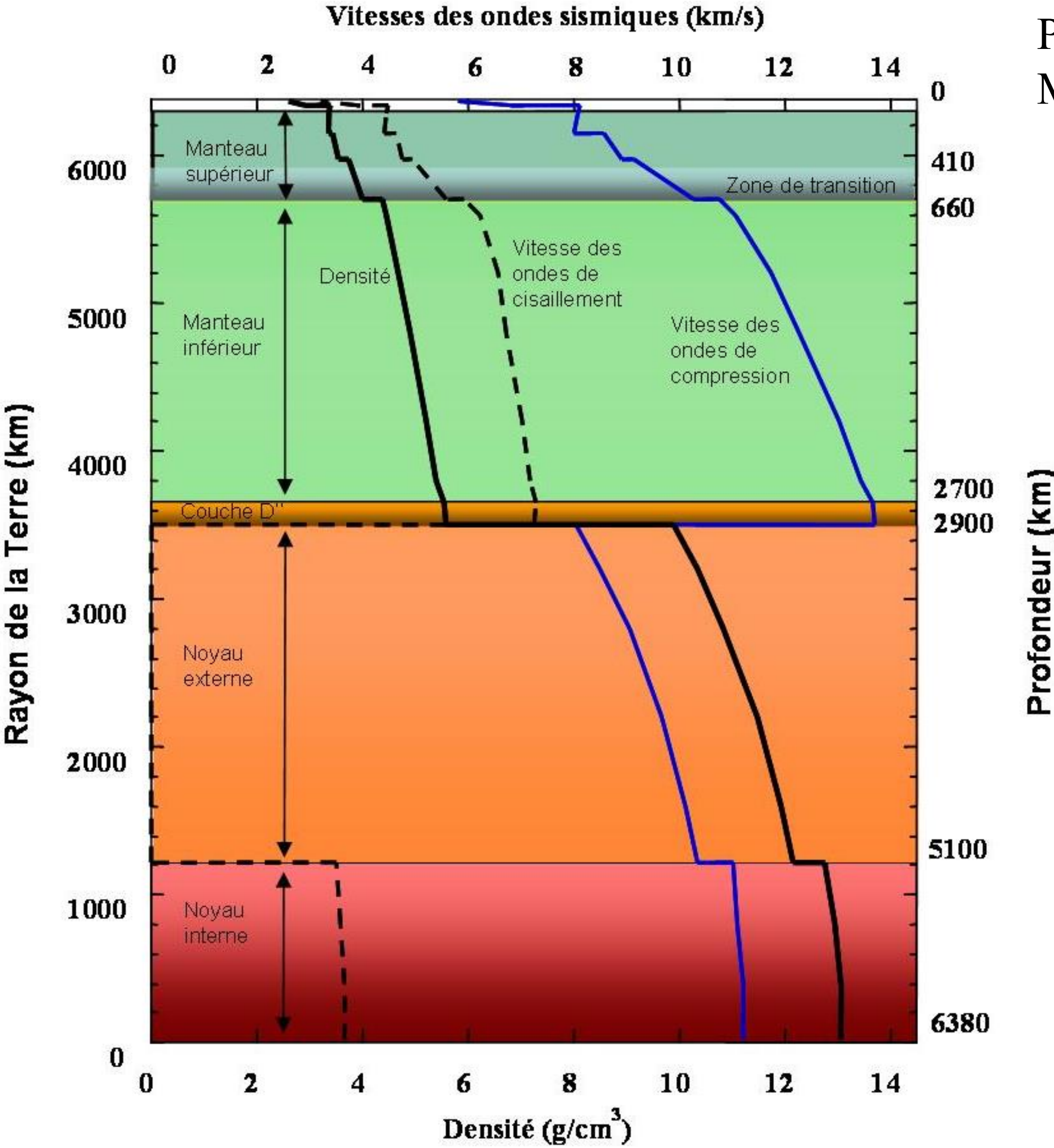

Preliminary Reference Earth Model: PREM

$$V_S = \sqrt{\frac{m}{r}}$$

$$V_P = \sqrt{\frac{K + \frac{4}{3}m}{r}}$$

μ : module de cisaillement

ρ : densité

K : module d'incompressibilité

Le Geotherme

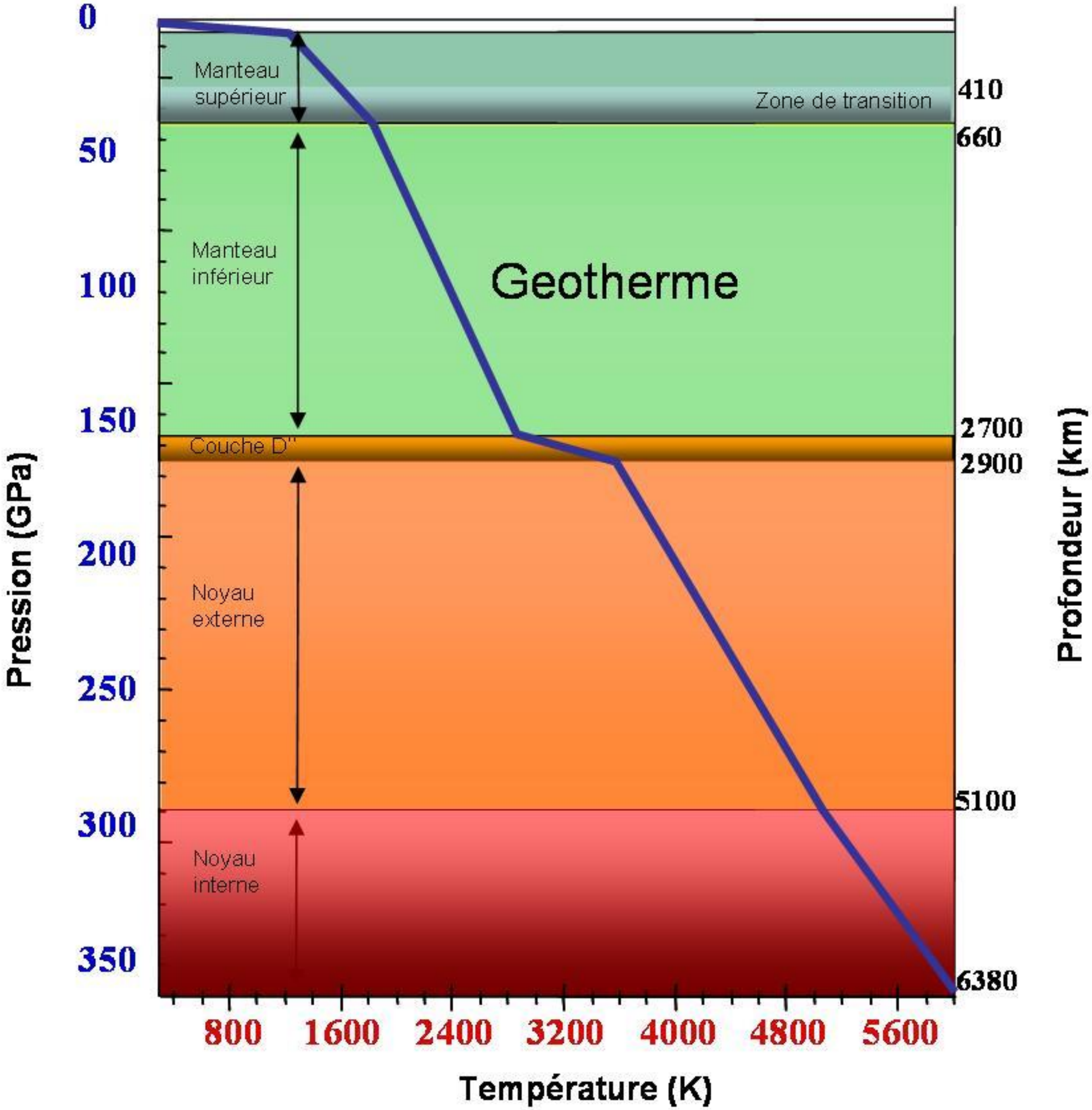

P (Pa) = Rho*G*h

Primordial heat
Radioactive decay

Radiation
Conduction
Convection / advection

Oceans: 25-38 mW.m-2

Continents: 21-34 mW.m-2

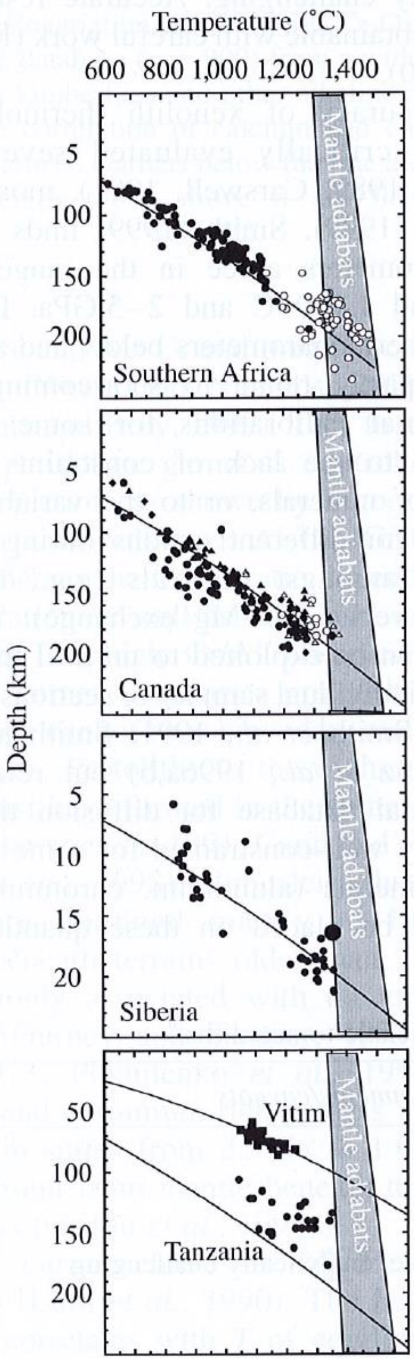

Figure 6 *P–T* arrays compiled for garnet peridotite xenoliths from several suites using two-pyroxene thermometry and Al-in-orthopyroxene barometry (T_{BKN} and P_{BKN} methods, Table 5). Data sources given in Rudnick and Nyblade with additional data here for Vitim (Ionov *et al.*, 1993a) and Canada (MacKenzie and Canil, 1999; Schmidberger and Francis, 1999). The best-fit line for the Kaapvaal data is plotted in each figure for reference. Intersection of *P–T* array with mantle adiabats (shaded field) represents an estimate of the thickness of lithosphere at the time of sampling.

Treatise on Geochem.

J.D. Winter *(Book)*

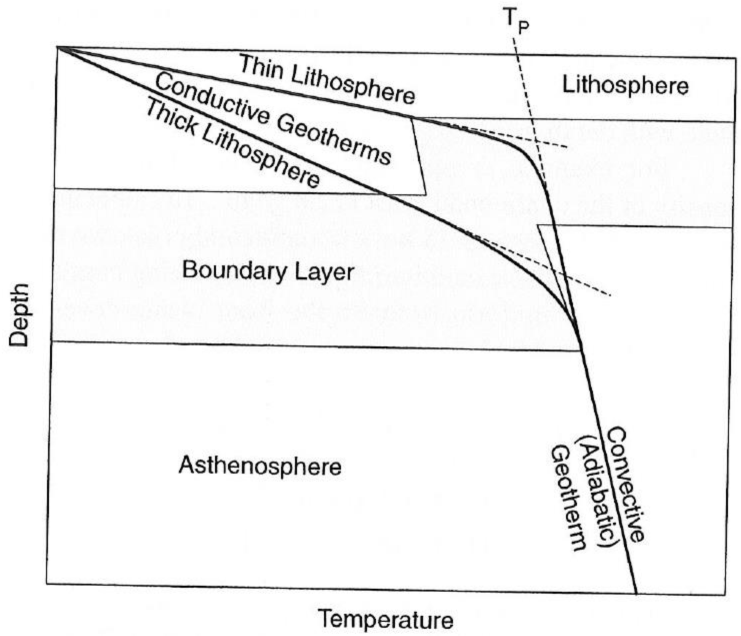

FIGURE 9 Diagrammatic cross-section through the upper 200 to 300 km of the Earth, showing geothermal gradients reflecting more efficient adiabatic (constant heat content) convection of heat in the mobile asthenosphere (steeper gradient) and less efficient conductive heat transfer through the more rigid lithosphere (shallower gradients). The boundary layer is a zone across which the transition in rheology and heat transfer mechanism occurs. The thickness of the boundary layer is exaggerated here for clarity: it is probably less than half the thickness of the lithosphere. Notice that thinner lithosphere (on right) allows convective heat transfer to shallower depths, resulting in a higher geothermal gradient (greater change in temperature for a given pressure increment) across the boundary layer and lithosphere. T_P is the *potential temperature*: the temperature that the deep solid mantle would attain at atmospheric pressure as extrapolated adiabatically to the surface (McKenzie and Bickle, 1988).

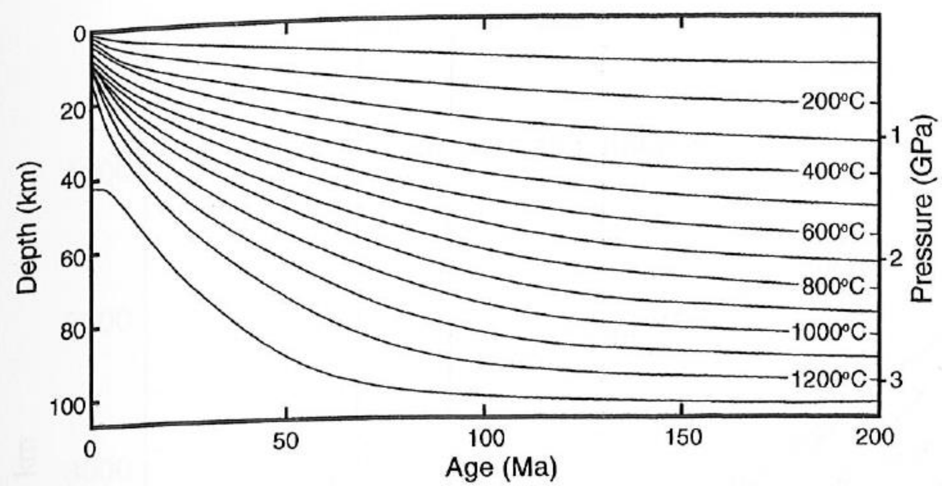

FIGURE 10 Temperature contours calculated for an oceanic plate generated at a mid-ocean ridge (age 0) and thickening as it cools. The 1300°C isotherm is a reasonable approximation for the base of the oceanic lithosphere. The plate thus thickens rapidly from zero to 50 Ma and is essentially constant beyond 100 Ma. From McKenzie et al. (2005).

J.D. Winter *(Book)*

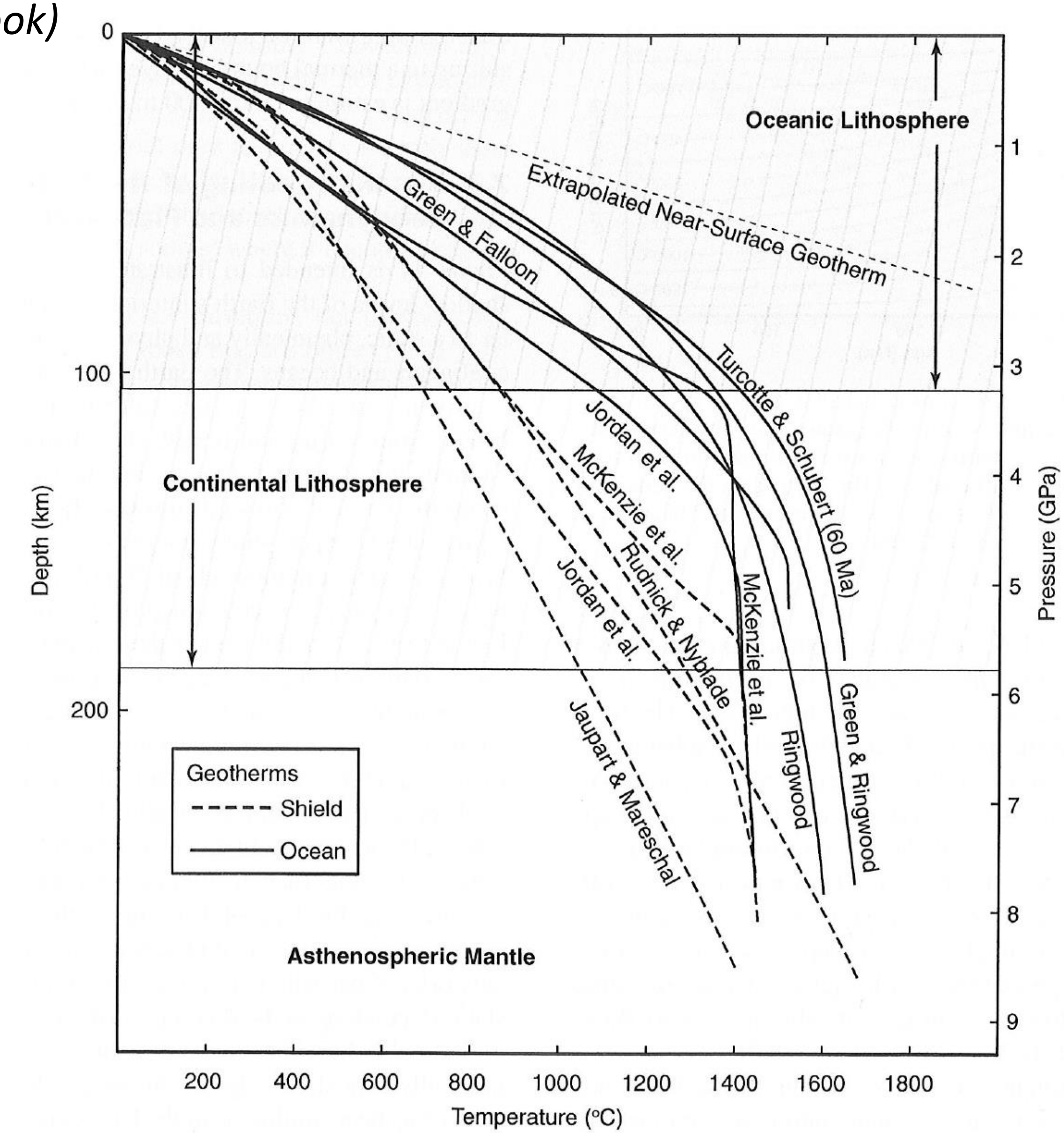

FIGURE 11 Estimates of oceanic (solid curves) and continental shield (dashed curves) geothermal gradients to a depth of 300 km. The thickness of mature (> 100Ma) oceanic lithosphere is shaded, and that of continental shield lithosphere is hatched. Data from Green and Falloon (1998), Green and Ringwood (1963), Jaupart and Mareschal (1999), McKenzie et al. (2005 and personal communication), Ringwood (1966), Rudnick and Nyblade (1999), and Turcotte and Schubert (2002).

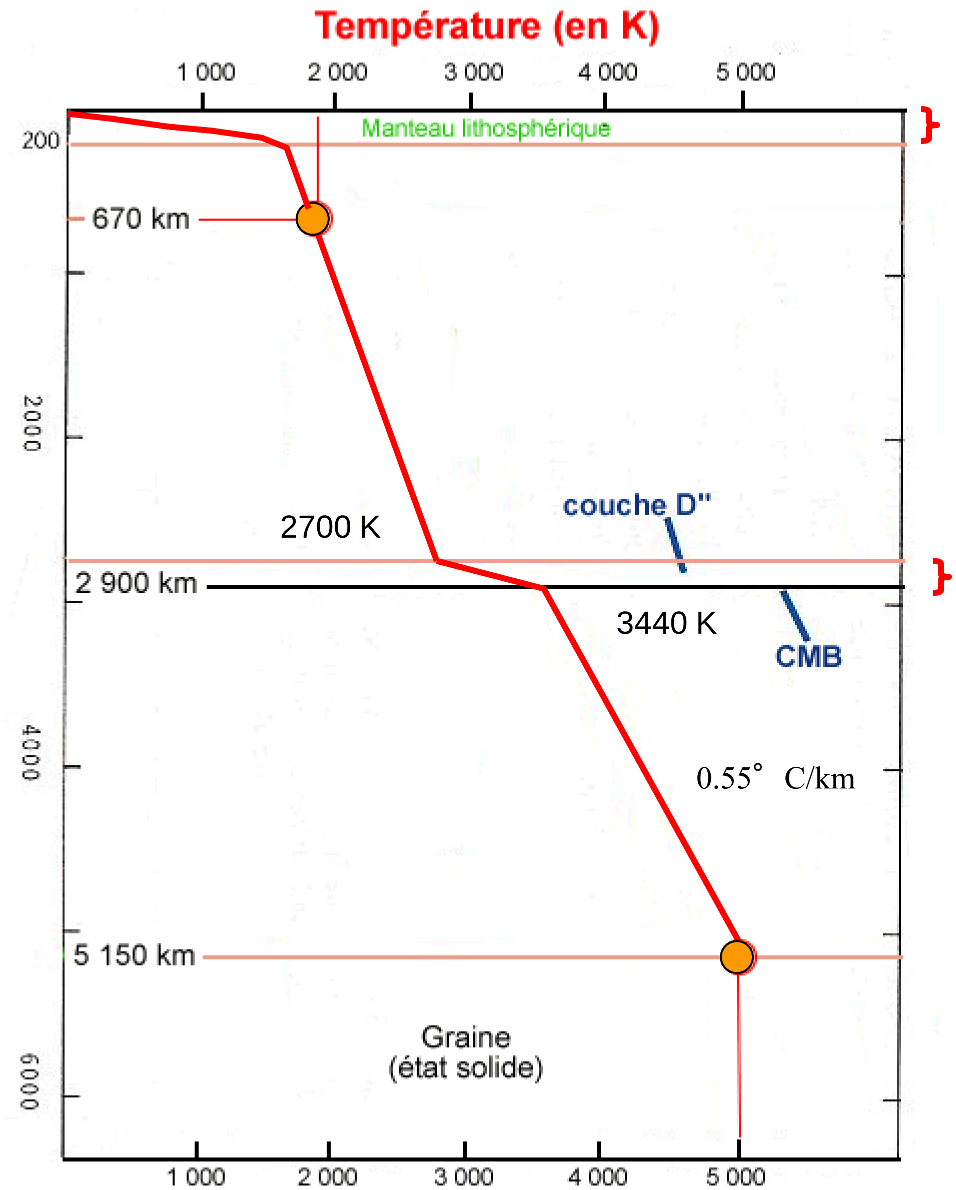

Couche limite thermique
diffusion

convection

Couche limite thermique
diffusion

J.D. Winter *(Book)*

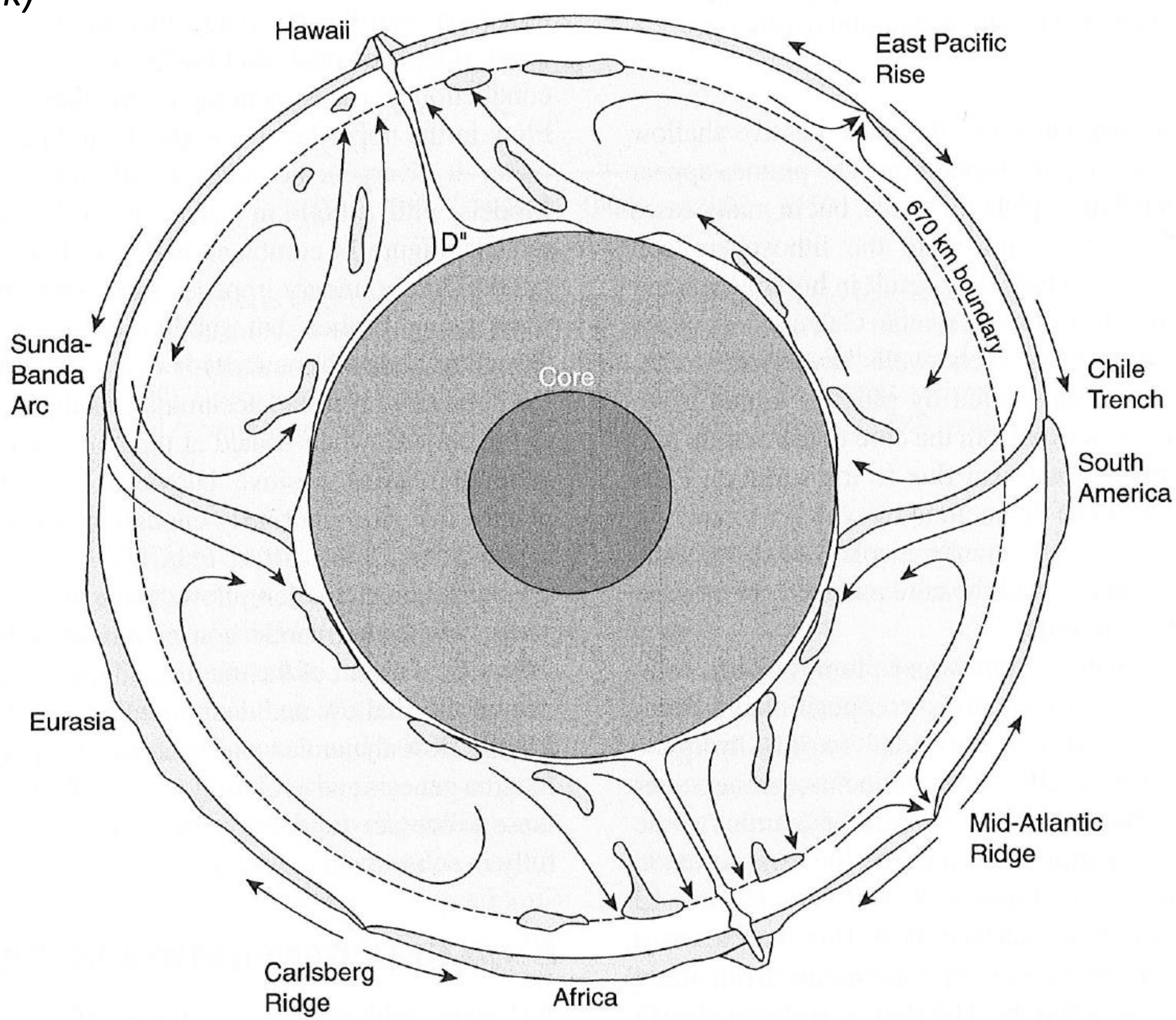

FIGURE 14 Schematic diagram of a two-layer dynamic mantle model in which the 660-km transition is a sufficient density barrier to separate lower mantle convection (arrows represent flow patterns) from upper mantle flow, largely a response to plate separation. The only significant things that can penetrate this barrier are vigorous rising hotspot plumes and subducted lithosphere (which sink to become incorporated in the D" layer, where they may be heated by the core and return as plumes). After Silver et al. (1988).

Minéralogie

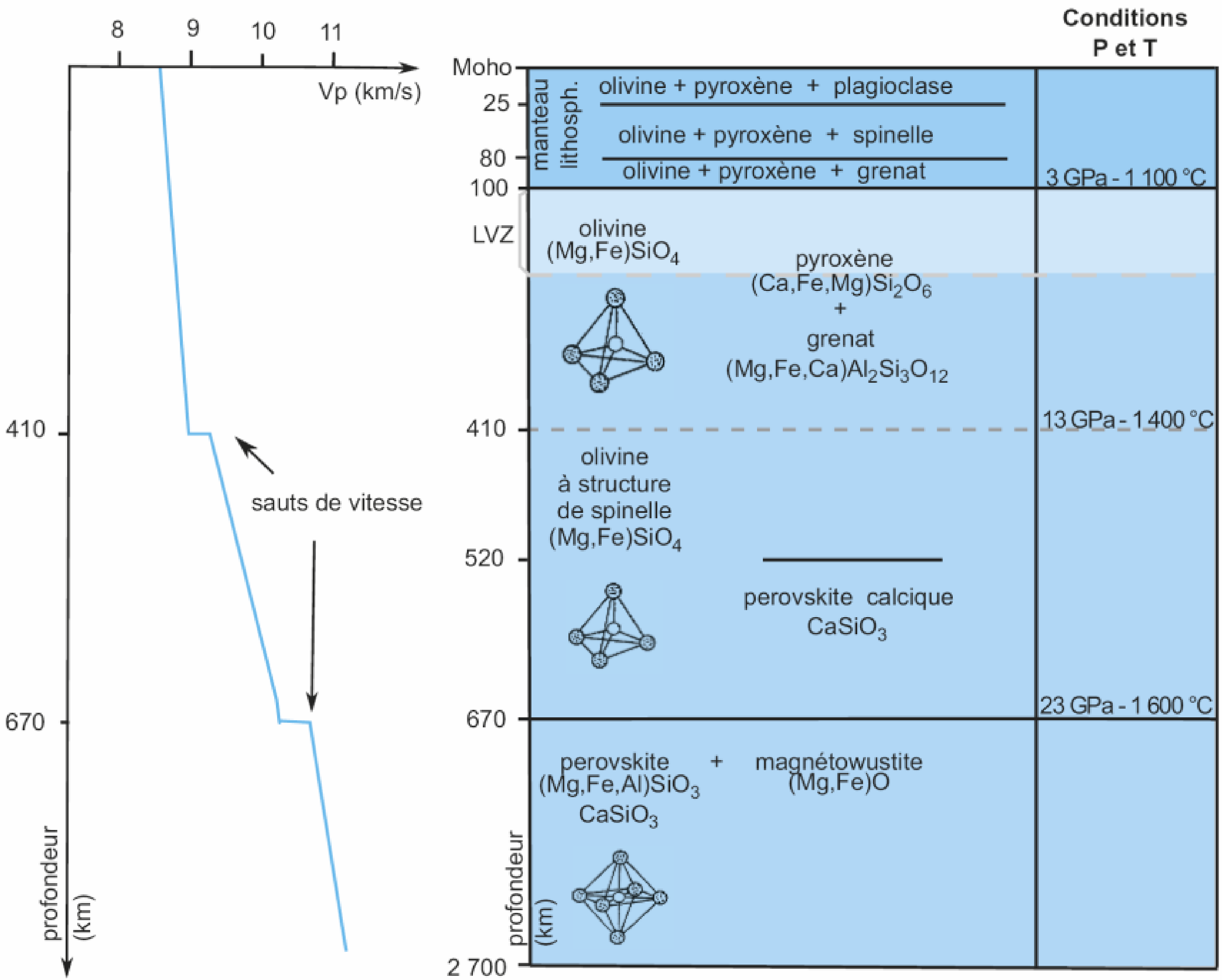

Figure 2.14 Modèle minéralogique pour le manteau déduit de l'échantillonnage, des données sismologiques et des études de laboratoire.

Peycru (Geol tt-en-1)

Mto Sup:
Ech + Expe + Sismo

Mto Inf:
Expe + Sismo

Minéralogie

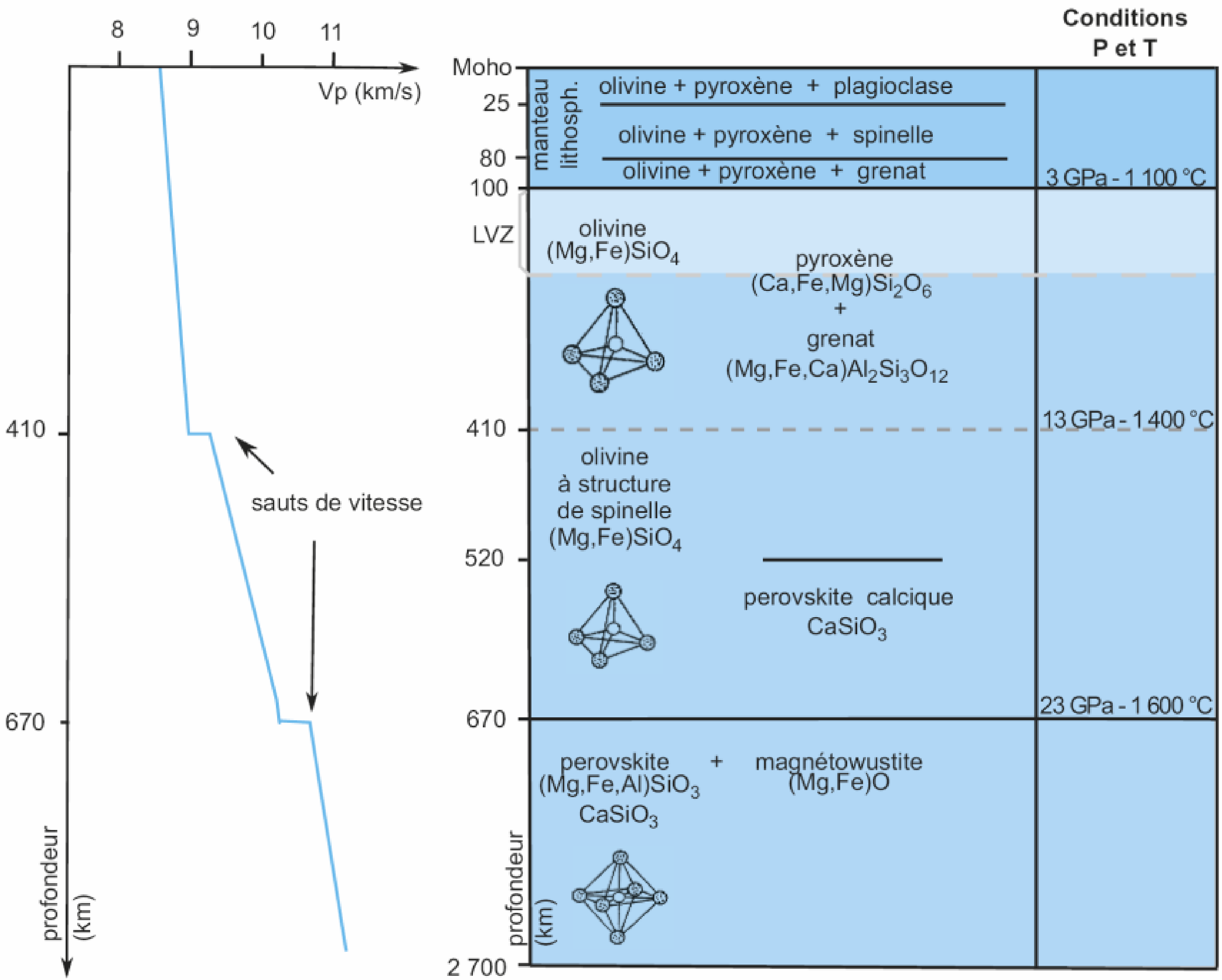

Figure 2.14 Modèle minéralogique pour le manteau déduit de l'échantillonnage, des données sismologiques et des études de laboratoire.

Peycru (Geol tt-en-1)

Mto Sup:
Ech + Expe + Sismo

Mto Inf:
Expe + Sismo

Presse multi-enclume

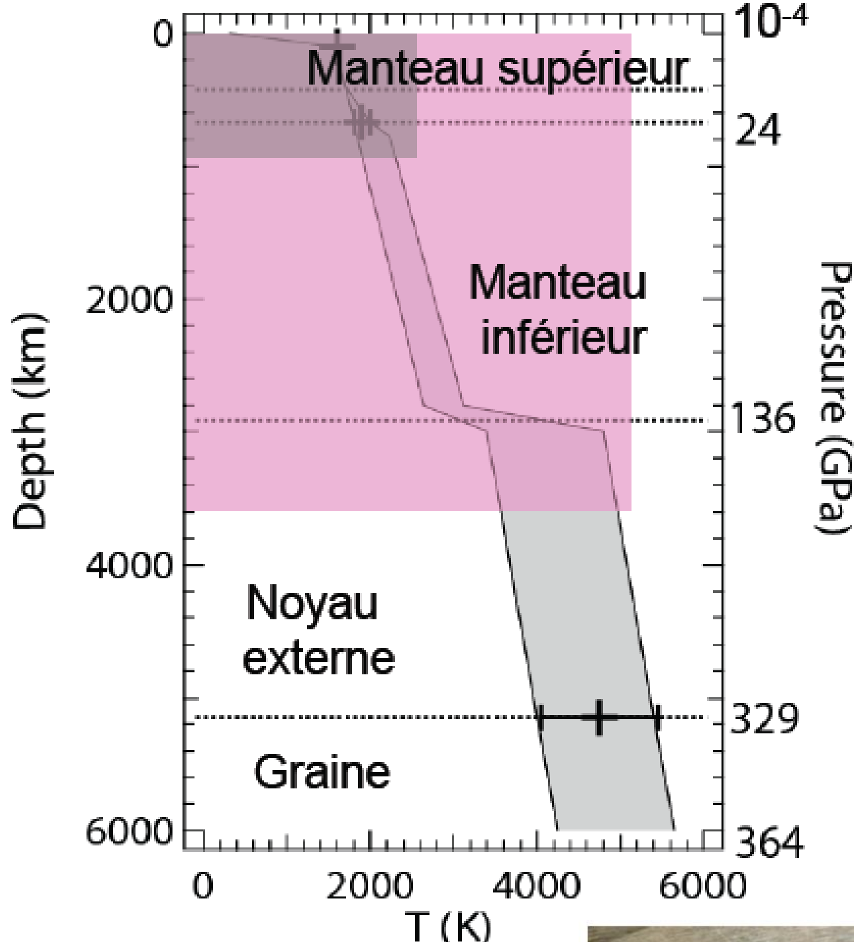

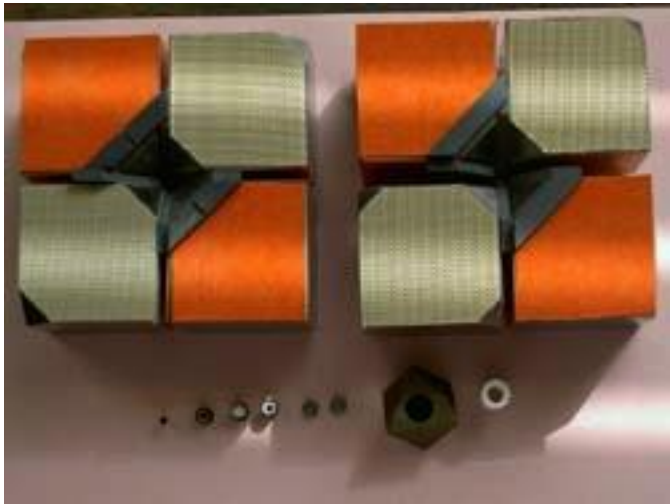

Presse enclume diamant

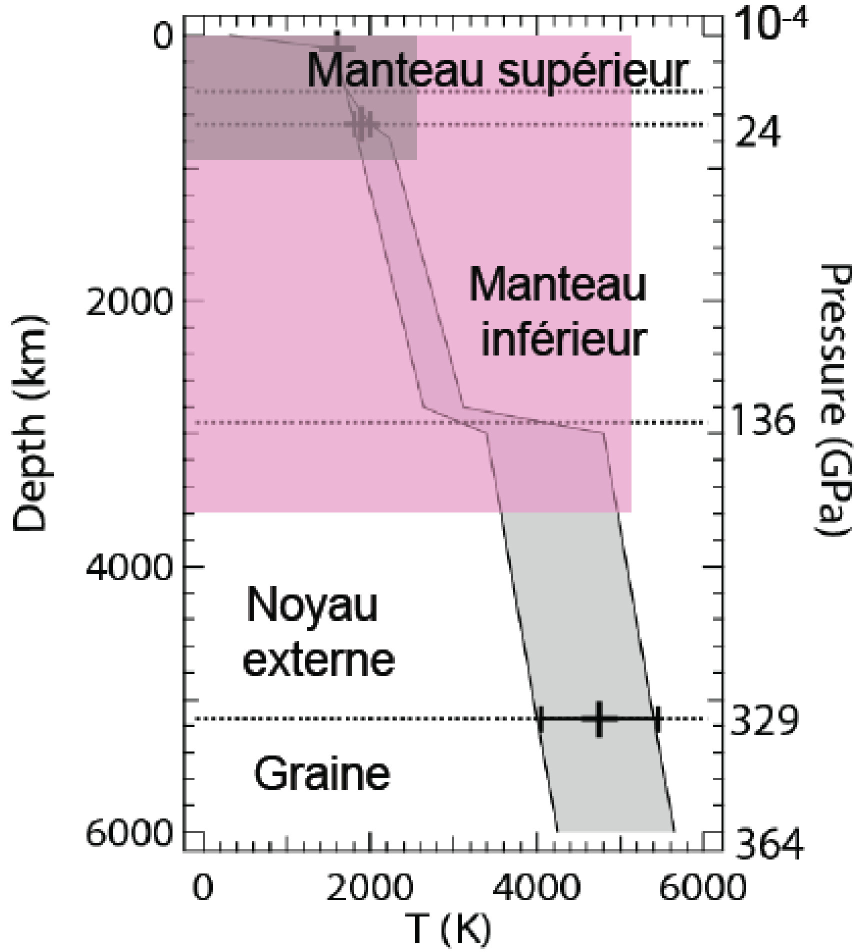

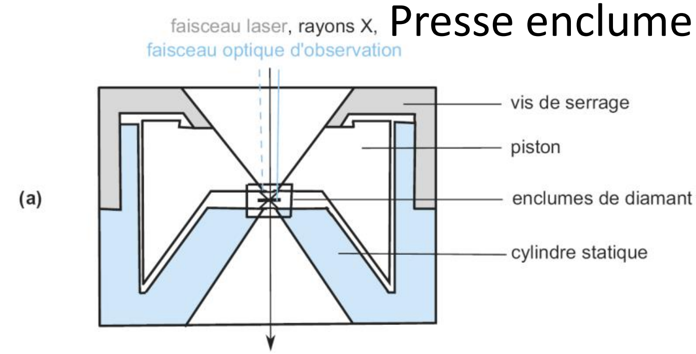

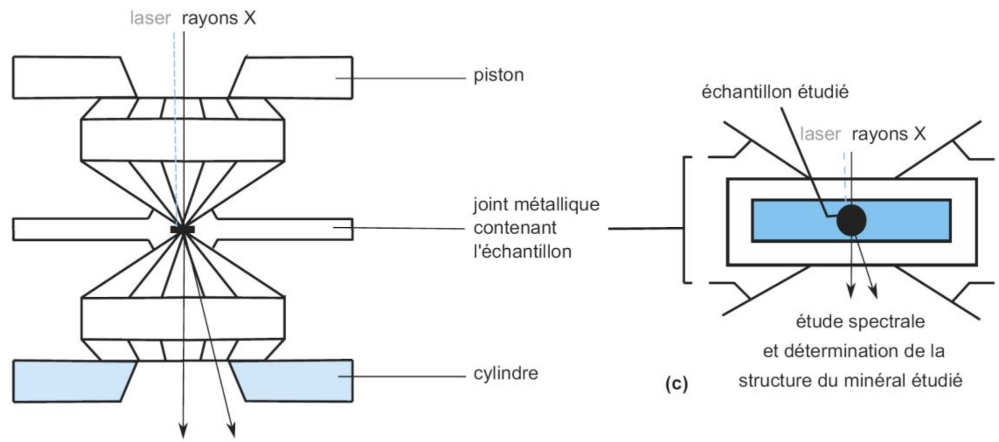

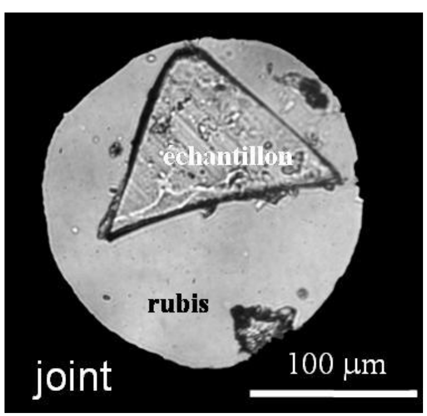

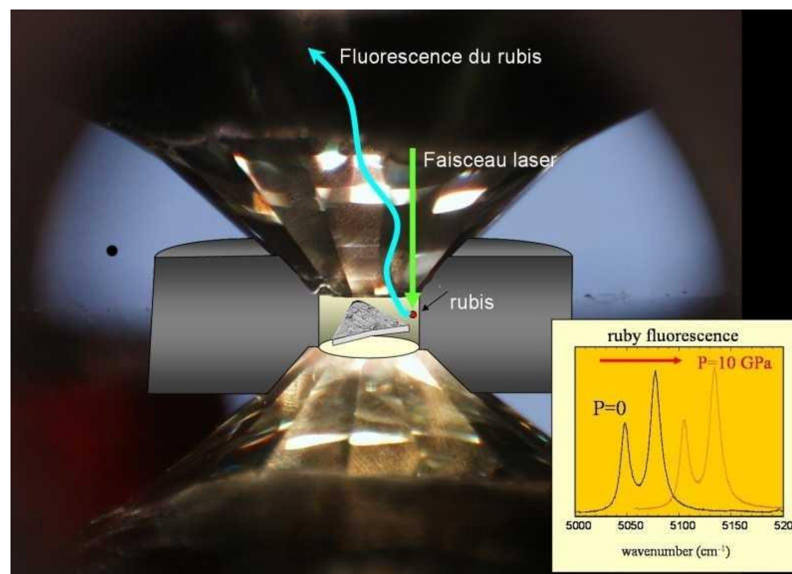

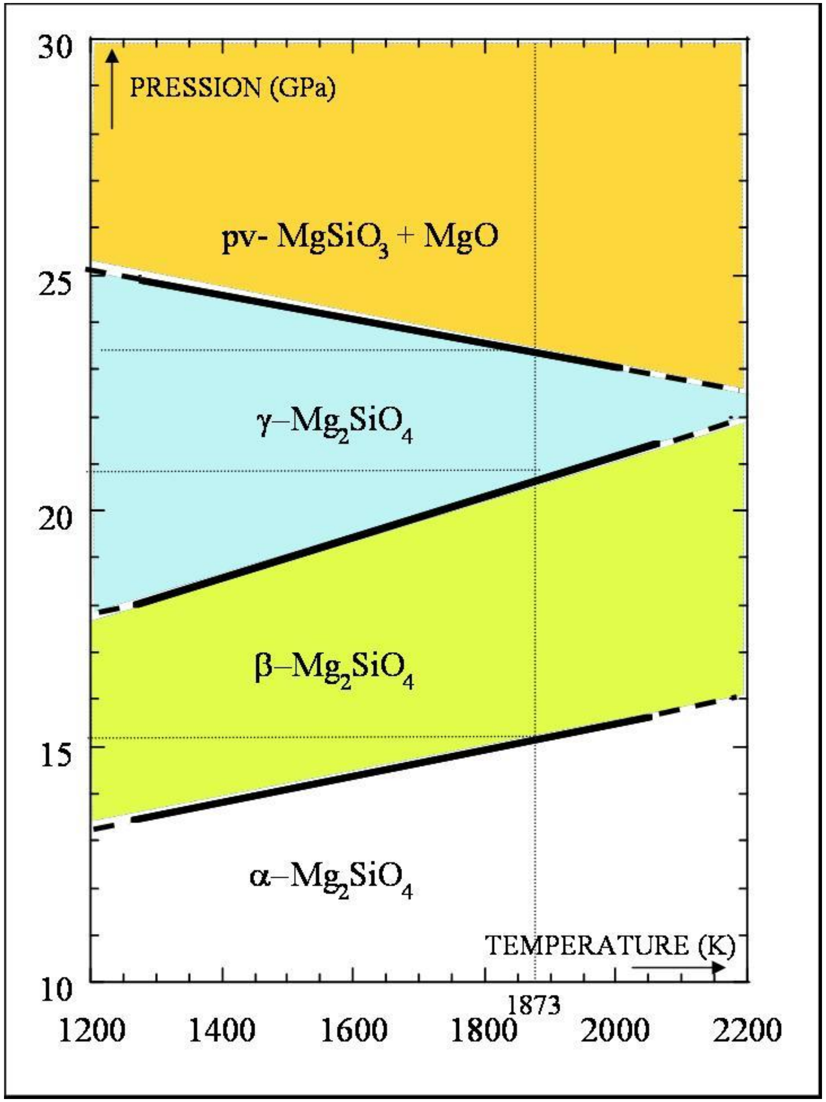

Mg_2SiO_4

Olivine (phase α) -->

wadsleyite (phase β) vers 410 km -->
ringwoodite (phase γ) vers 520 km -->
« perovskite » (Mg, Fe)SiO3 + périclase (MgO) vers 66O km

"olivine-spinelle" correspond à wadsleyite + ringwoodite

Perovskite: $CaTiO_3$

Spinelle:$MgAl_2O_4$

Diagramme de phase de Mg_2SiO_4
Avec la pression la forstérite, Mg_2SiO_4 (α-Mg_2SiO_4), se transforme successivement :
en phase β-Mg_2SiO_4 de (structure spinelle modifié)
puis en γ-Mg_2SiO_4 (de structure spinelle)
puis en un assemblage de pv-$MgSiO_3$ (de structure perovskite)+ MgO (périclase)

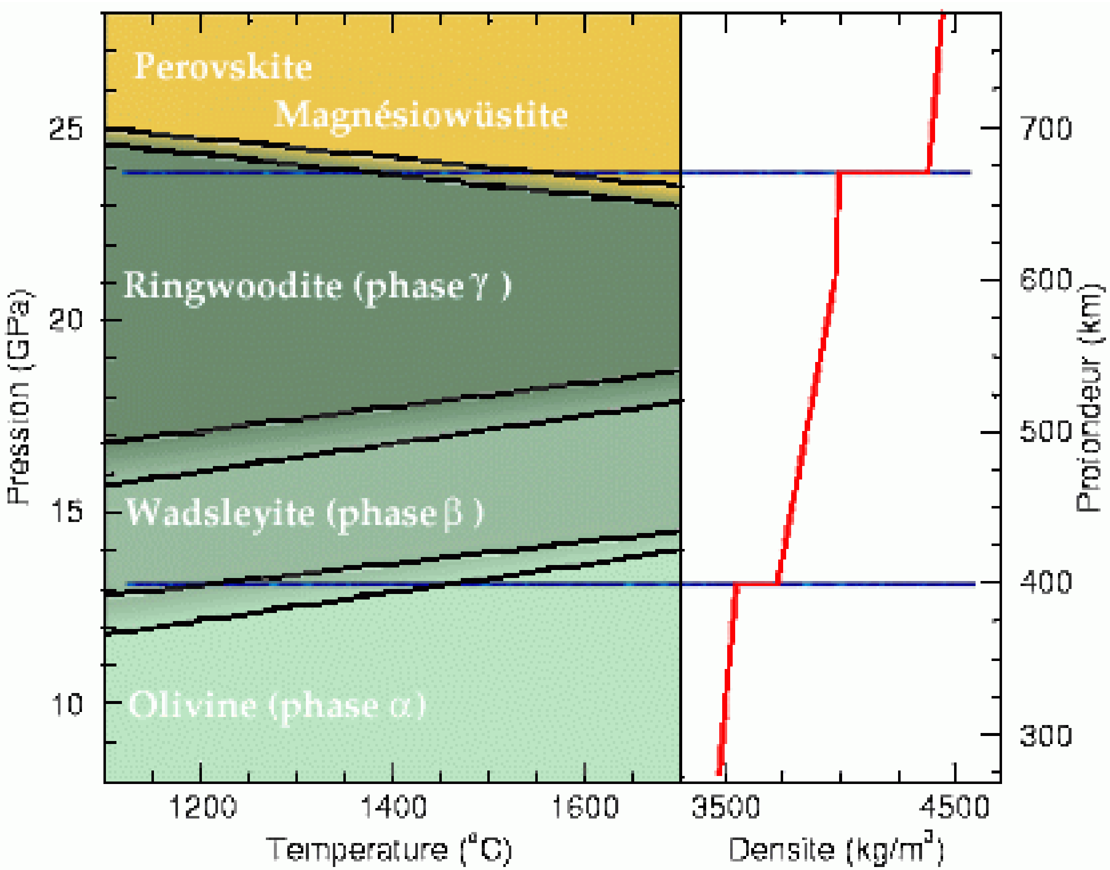

Minéral	$V_{molaire}$ (cm^3/mol)
α-Mg_2SiO_4	43.67
β-Mg_2SiO_4	40.54
γ-Mg_2SiO_4	39.65
$MgSiO_3$ perovskite	24.42
MgO	11.25

$(Mg_{0.9}Fe_{0.1})_2SiO_4$

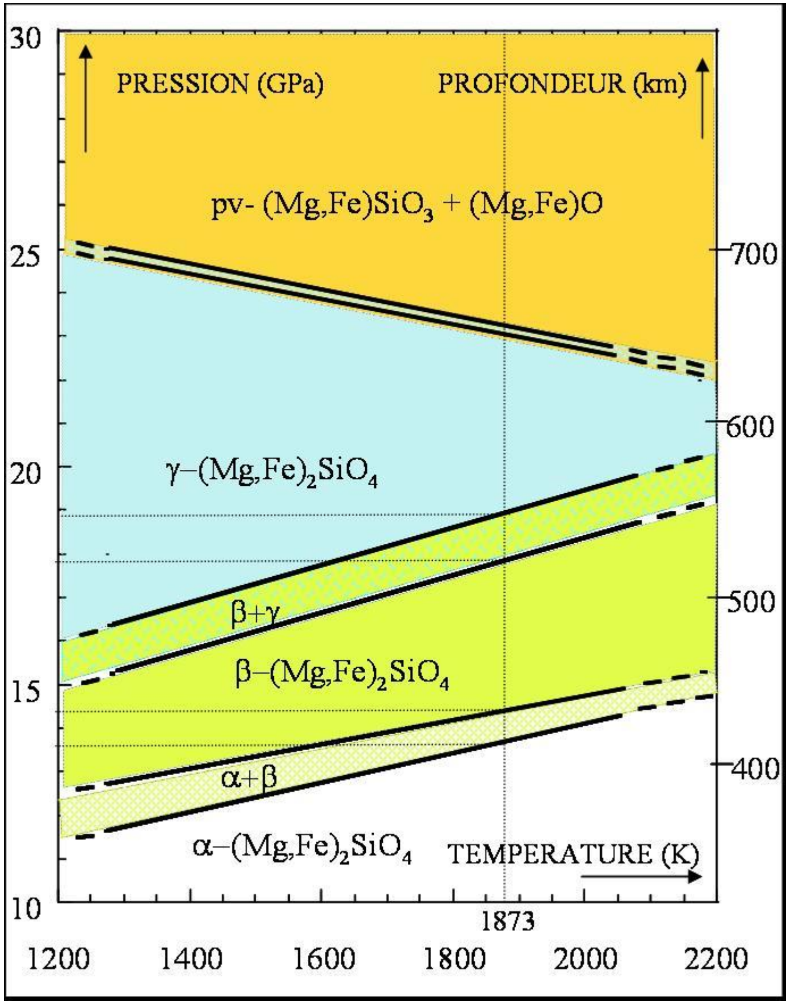

Magnésiowustite: (Mg, Fe)O

Diagramme de phase de $(Mg_{0.9},Fe_{0.1})_2SiO_4$.
La présence de fer conduit, non plus à des limites franches entre les différentes phases,
mais à des domaines de coexistence sur des intervalles plus ou moins larges de pression et température.

J.D. Winter *(Book)*

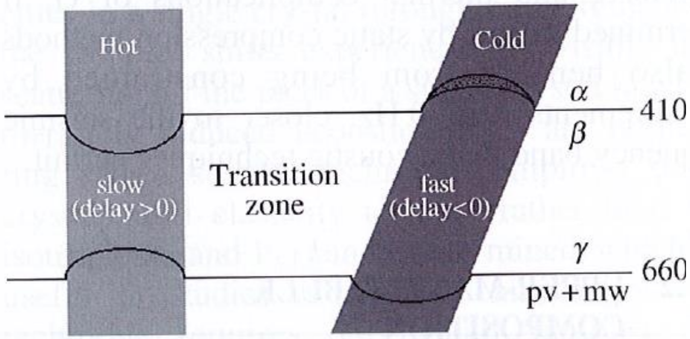

Figure 2 Schematic illustration of thermal contr
olivine phase transformations in the transition z
showing perturbations to transition zone thickr
transition zone seismic velocities (delay times),
depths of individual phase transformations.

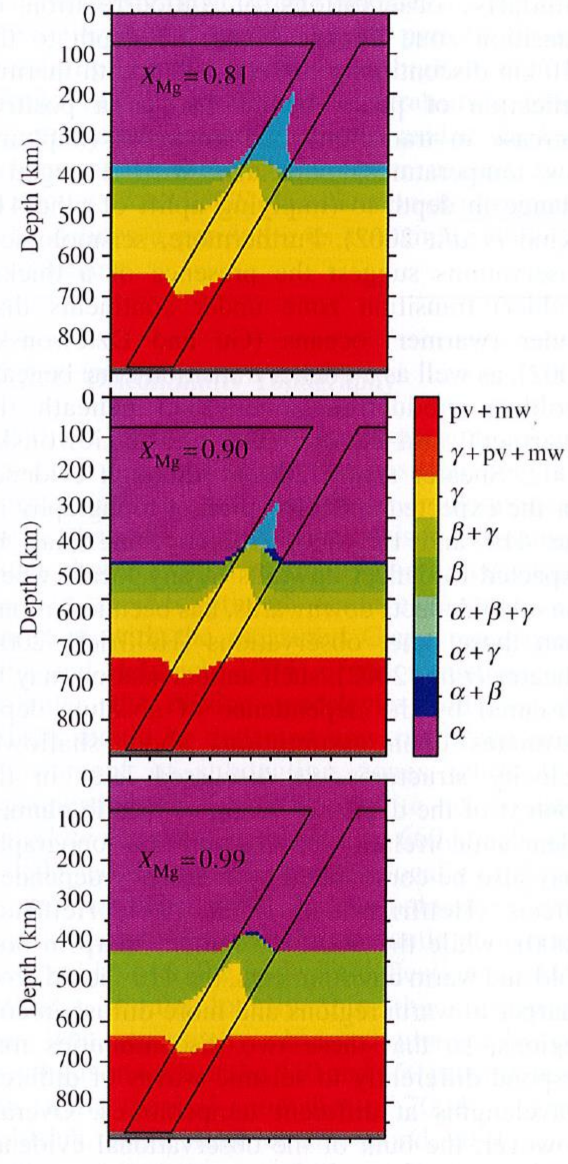

Figure 4 Effects upon olivine phase equilibria of variations in Mg/(Mg + Fe) for pyrolite (center), Fe enrichment (top), and Mg enrichment (bottom) (vertical resolution is 10 km).

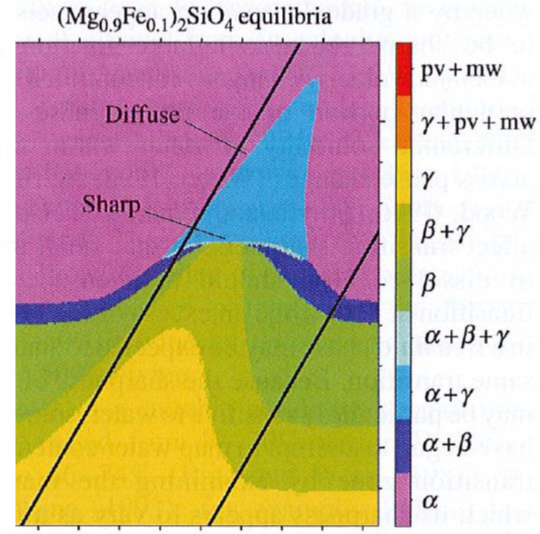

3 Effects upon olivine phase equilibria near
depth of low temperatures in subduction zones,
eral thermodynamic parameters of Fei *et al.*
Dark lines denote boundaries of subducting
ıases are: (α) olivine, (β) wadsleyite, (γ)
dite, (mw) magnesiowüstite, and (pv) ferro-
an silicate perovskite. Note that the $\alpha \rightarrow \beta$
ın near 410 km is first uplifted and then
ɛs into a strongly uplifted diffuse $\alpha \rightarrow \alpha + \gamma$
n overlying a weakly uplifted sharp boundary
ɪr Bina, 2002) (vertical resolution is 1 km).

Treatise on Geochem.

Pyroxène: $MgSiO_3$

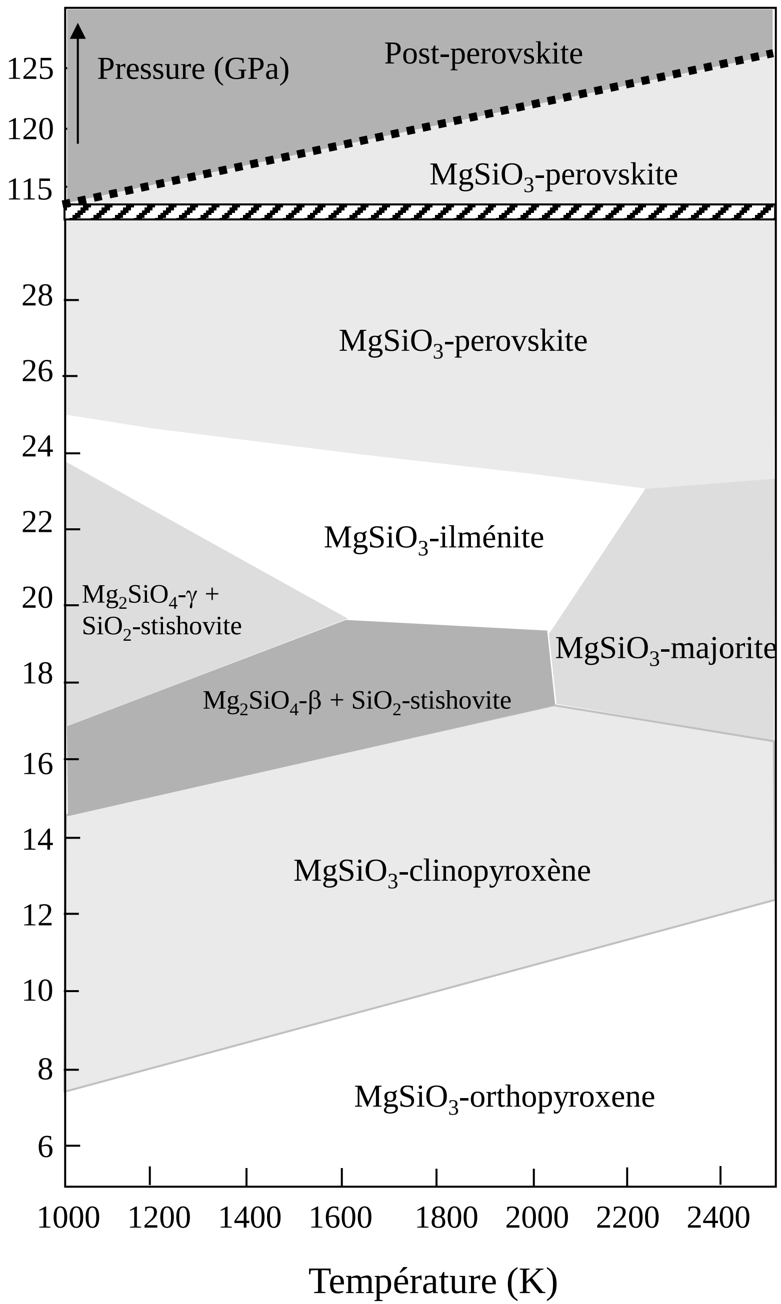

Diagramme de phase de $MgSiO_3$
En fonction de la pression et de la température on observe les minéraux suivants :

$MgSiO_3$ de structure orthopyroxène
$MgSiO_3$ de structure clinopyroxène
$MgSiO_3$ de structure ilménite
$MgSiO_3$ de structure majorite
$MgSiO_3$ de structure perovskite
$MgSiO_3$ de structure post-perovskite

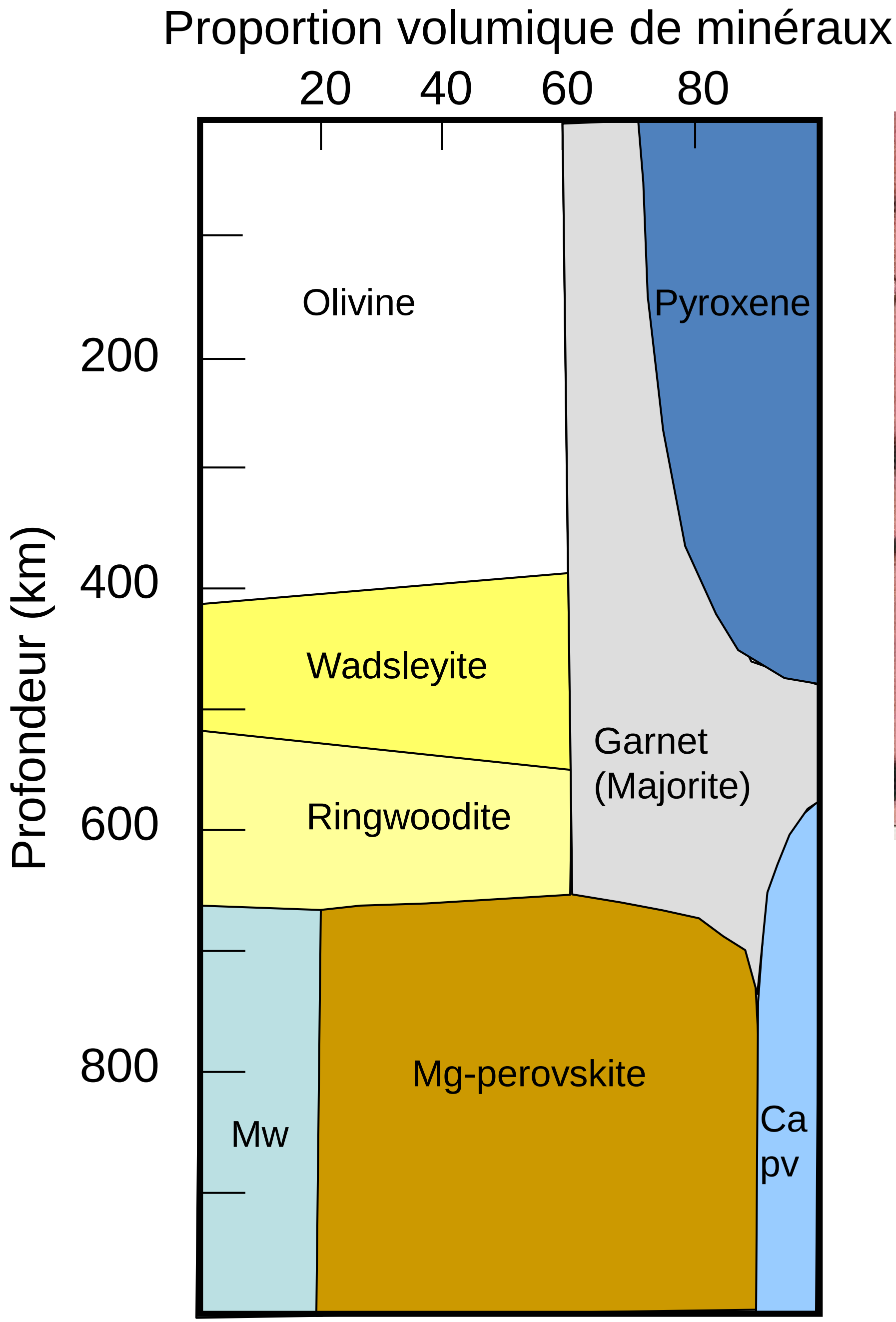
Proportion volumique de minéraux
20
40
60
80
Profondeur (km)
200
400
600
800
Olivine
Pyroxene
Wadsleyite
Garnet
(Majorite)
Ringwoodite
Mg-perovskite
Mw
Ca
pv

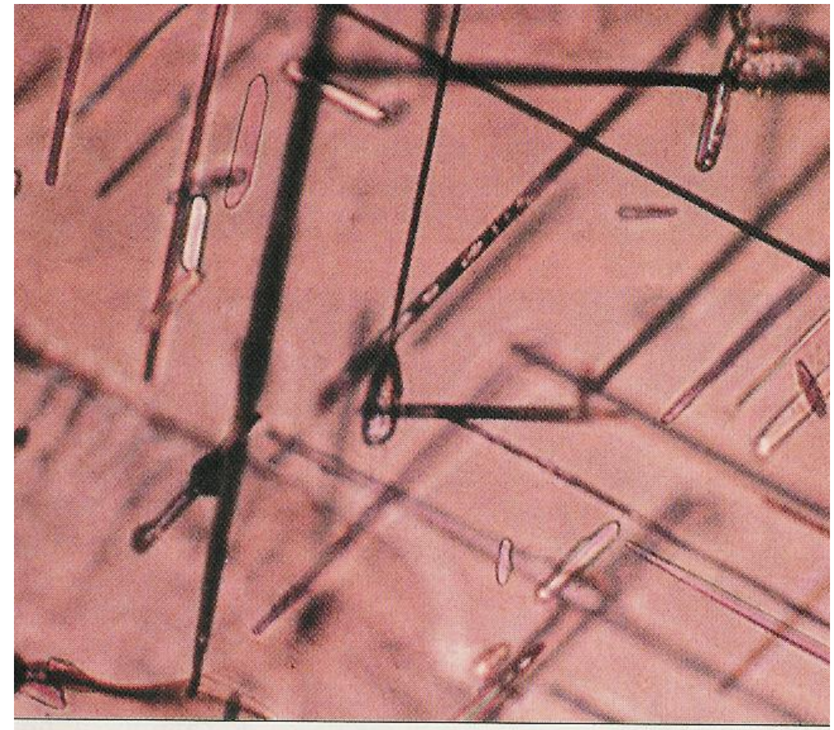

Minéralogie

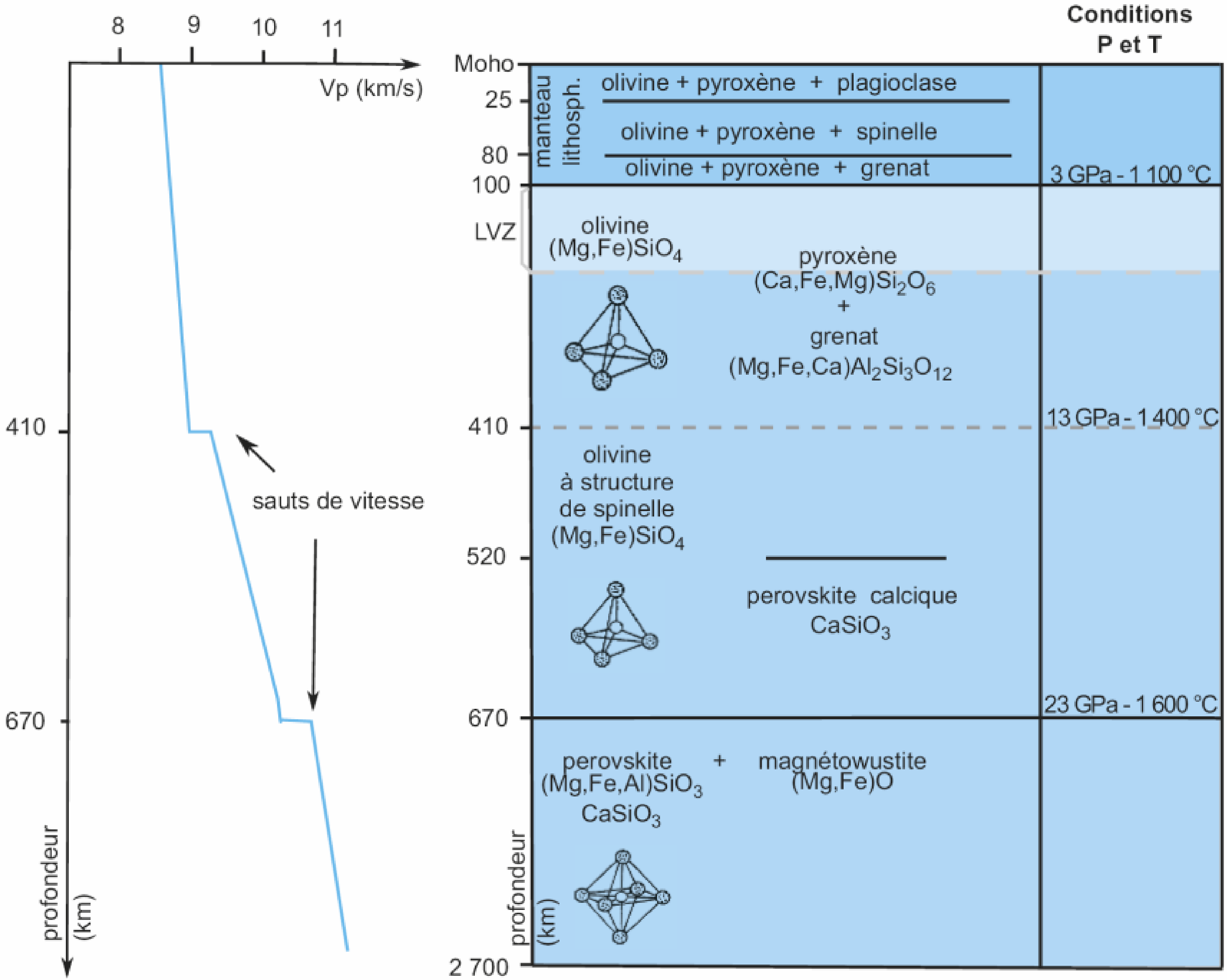

Figure 2.14 Modèle minéralogique pour le manteau déduit de l'échantillonnage, des données sismologiques et des études de laboratoire.

Peycru (Geol tt-en-1)

Mto Sup:
Ech + Expe + Sismo

Mto Inf:
Expe + Sismo

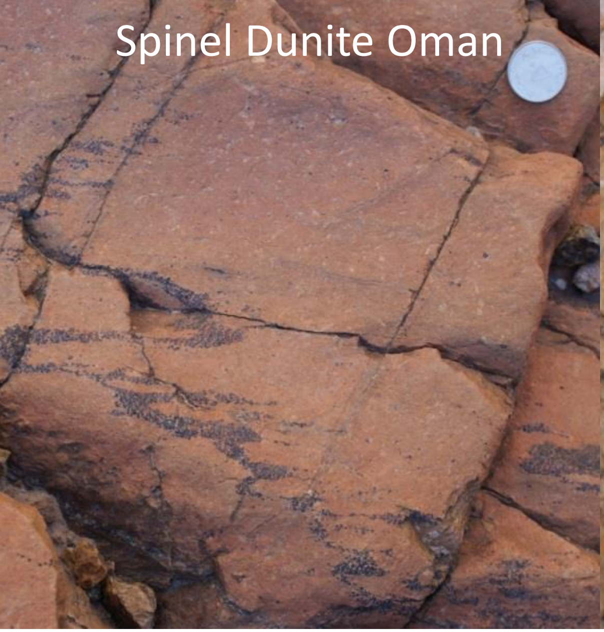
Spinel Dunite Oman


Lherzolite, Iran


Harzburgite, Oman


Plag. Peridotite, Makran Iran

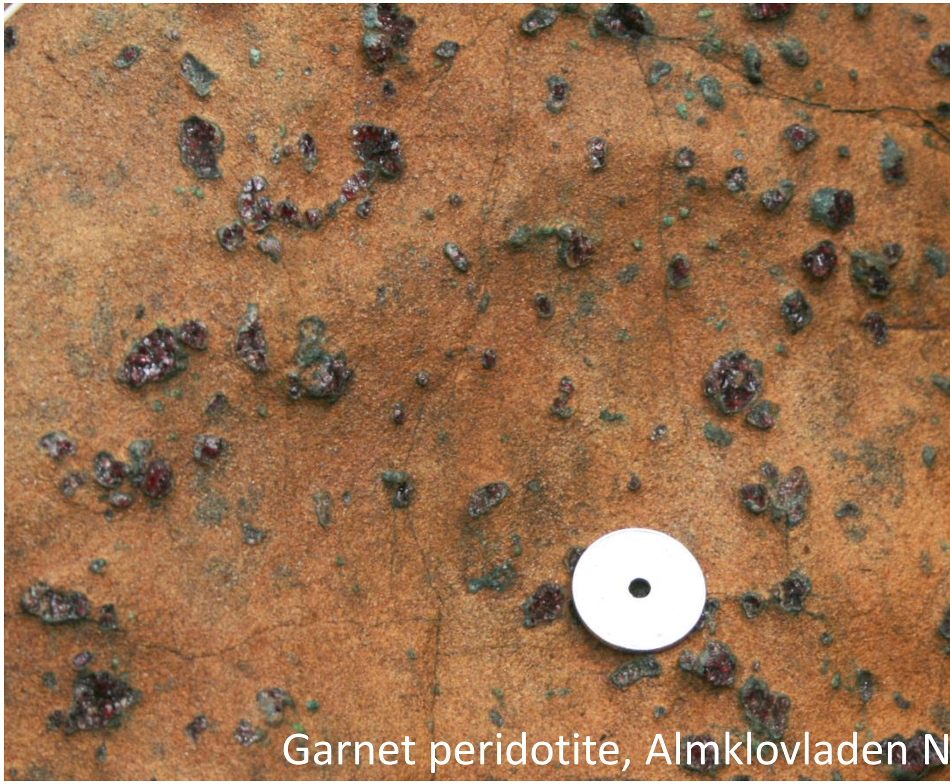
Garnet peridotite, Almklovladen N

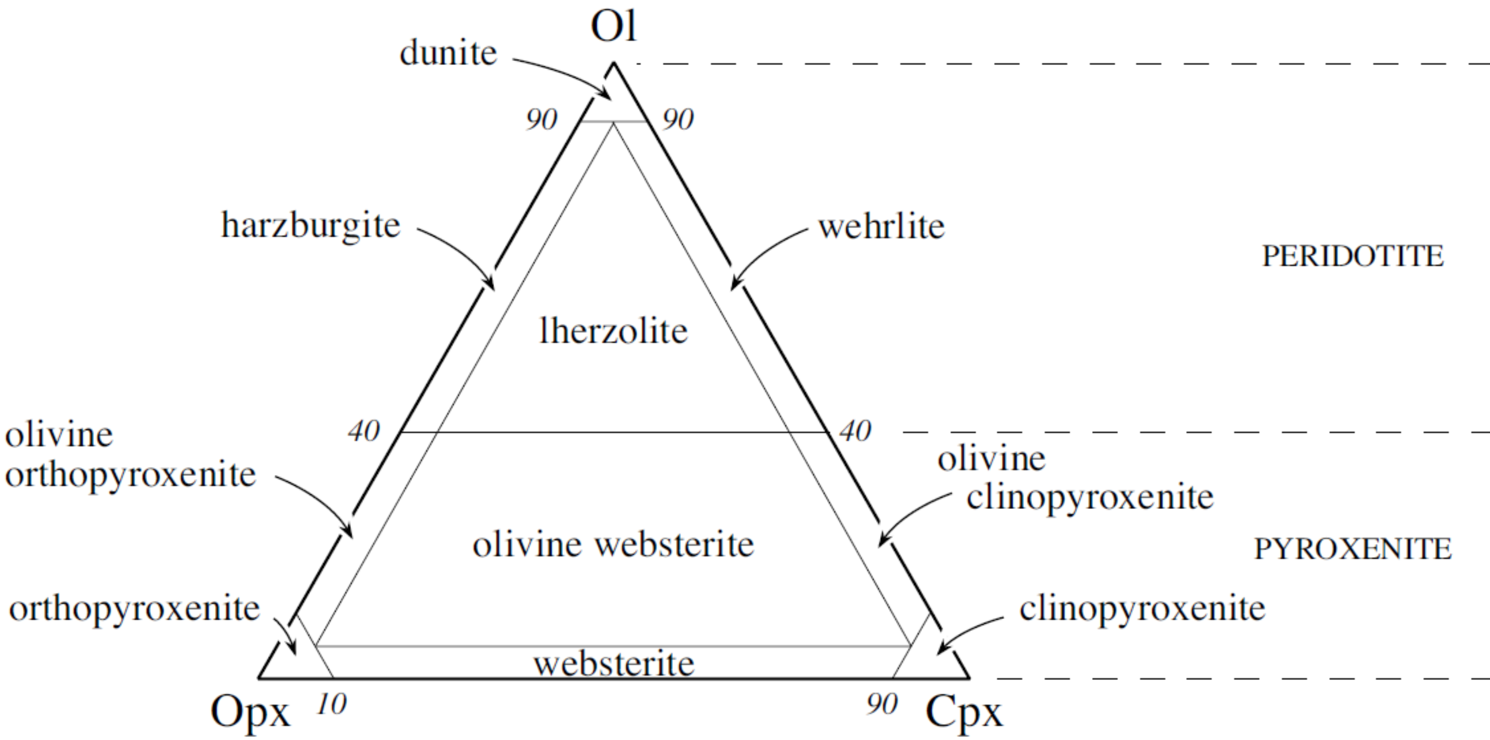

+ phase alumineuse:
Plagioclase / Spinelle / Grenat

Dunite
Harzburgite
Lherzolite

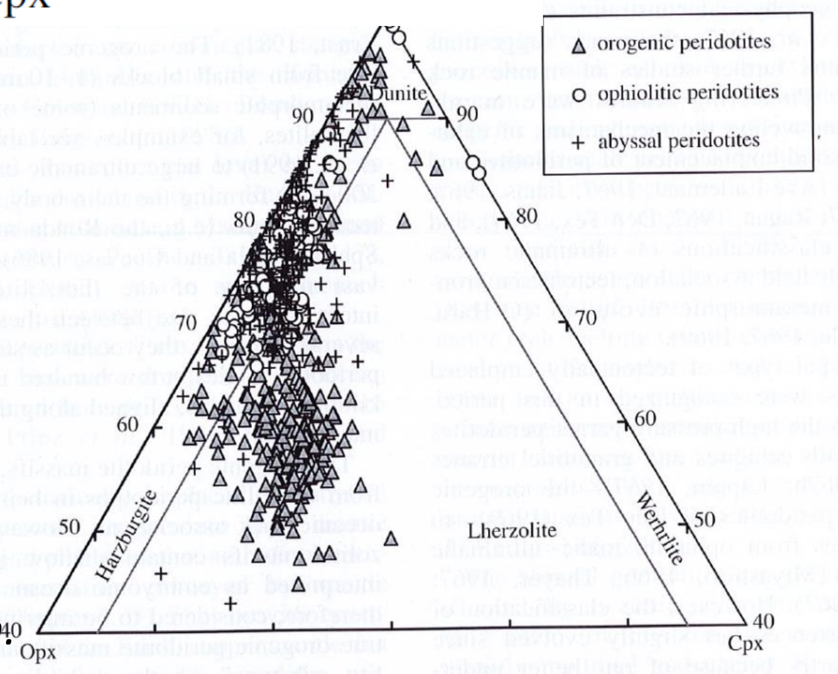

Treatise on Geochem.

Géochimie

Mineralogie = chimie

	Roche du manteau				Extract.		Principaux mineraux						
	Lhz	*Hz*	*Dun*		*Basalt*		*Ol*	*Opx*	*Cpx*	*An90*	*Sp(Lhz)*	*Sp(Dun)*	*Grt(Pyr)*
SiO2	42.3	39.9	38.3		50.5		40.5	55.2	50	44.2	-	-	42.7
Al2O3	4.2	2.3	1.4		14.7		-	3.8	7.2	35	58.5	29.7	21.2
FeO	9.8	11.4	12.6		10.4		9.8	6.6	3.1	-	12	17	8.6
MgO	31.2	33.2	37.9		7.6		48.7	33.8	15.4	-	20	17	20.7
CaO	5	2.9	1		11.4		-	0.5	20.1	18.6	-	-	4.3
Na2O	0.5	0.3	0.2		1.8		-	-	1.9	0.8	-	-	-
K2O	<0.1	<0.1	<0.1		0.2		-	-		-	-	-	-
Cr2O3	0.2	0.3	0.4		0.1		-	0.2	0.5	-	7.5	36	1.5
TiO2	0.6	0.3	0.1		1.68		-	0.1	0.5	-	0.1	0.1	0.8

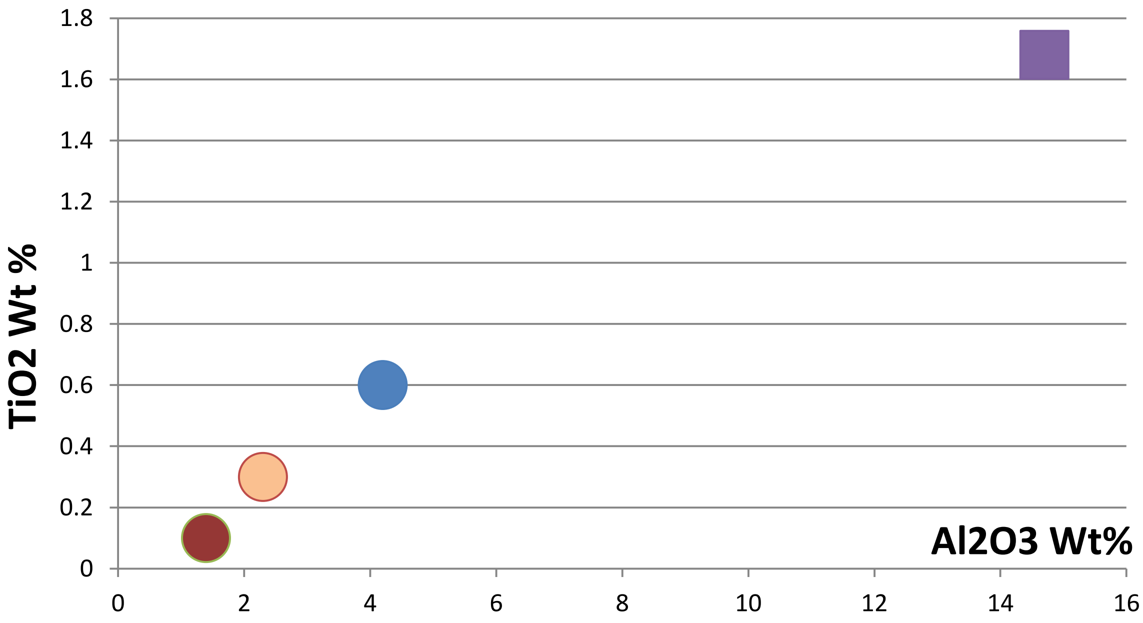

Simpliste... PREM

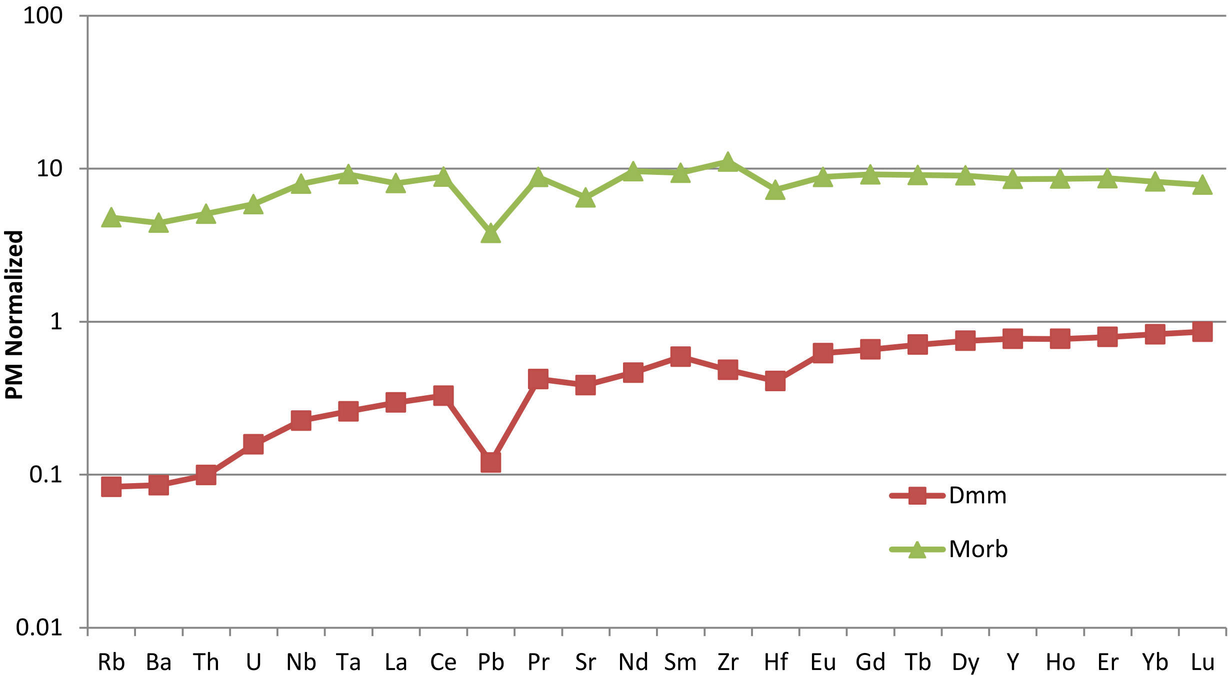

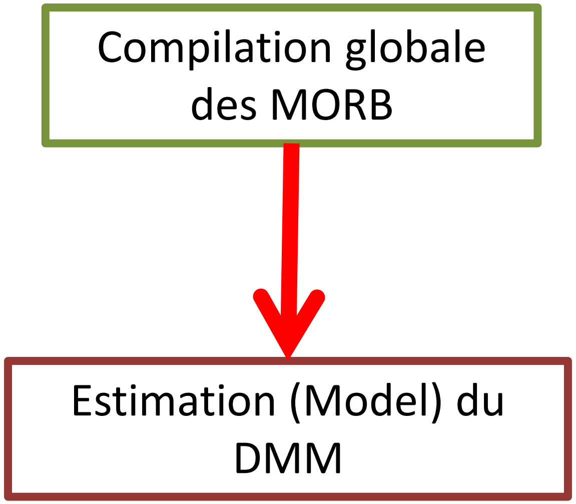

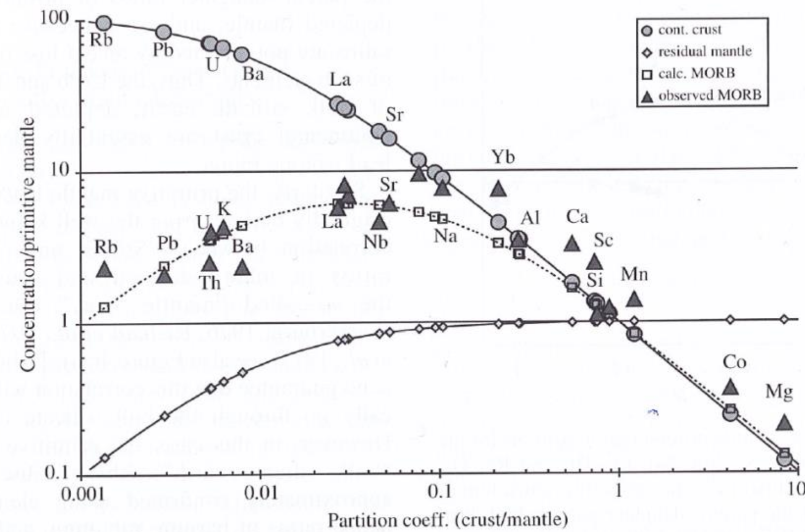

Figure 2 Comparison of the abundances of trace and (some) major elements in average continental crust and average MORB. Abundances are normalized to the primitive-mantle values (McDonough and Sun, 1995). The "partition coefficient" of each element is calculated by solving Equation (2) for D, using a melt fraction $F = 0.009$ and its abundance value in the continental crust (Rudnick and Fountain, 1995). The respective abundances in average MORB are plotted using the same value of D and using the average ("normal") MORB values of (Su, 2002), where "normal" refers to ridge segments distant from obvious hotspots.

Treatise on Geochem.

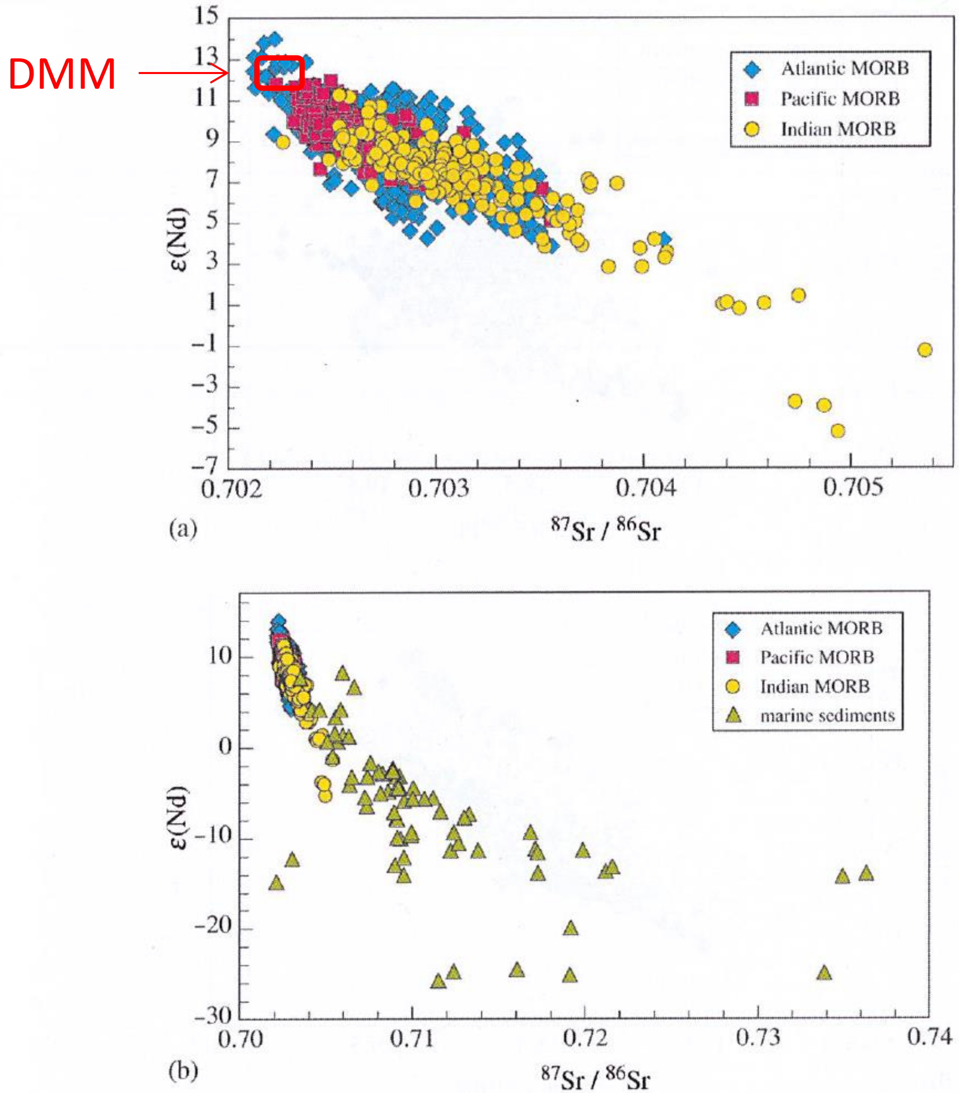

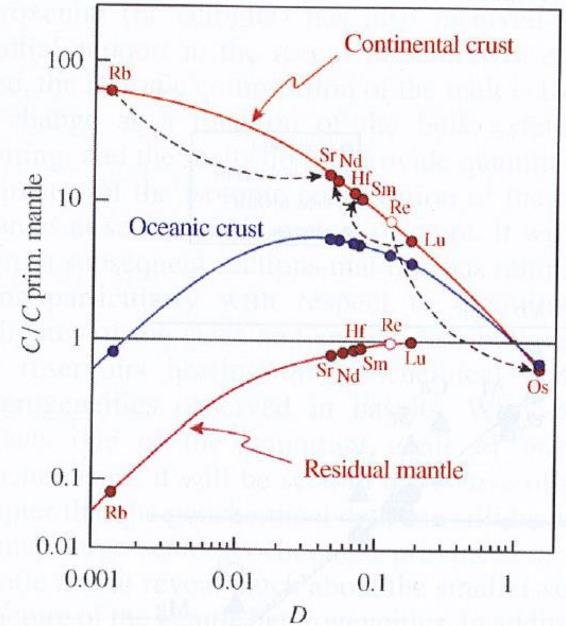

Figure 3 Crust–mantle differentiation patterns for the decay systems Rb–Sr, Sm–Nd, Lu–Hf, and Re–Os. The diagram illustrates the depletion-enrichment relationships of the parent–daughter pairs, which lead to the isotopic differences between continental crust and the residual mantle. For example, the Sm/Nd ratio is increased, whereas the Rb/Sr ratio is decreased in the residual mantle. This leads to the isotopic correlation in mantle-derived rocks plotted in Figure 4(a). The construction is similar to that used in Figure 2, but *D* values have been adjusted slightly for greater clarity.

Figure 4 (a) $^{87}Sr/^{86}Sr$ versus ε(Nd) for MORBs from the three major ocean basins. ε(Nd) is a measure of the deviation of the $^{143}Nd/^{144}Nd$ ratio from the chondritic value, assumed to be identical to the present-day value in the bulk silicate earth. It is defined as $\varepsilon(Nd) = 10^4 \times (^{143}Nd/^{144}Nd_{measured} - {}^{143}Nd/^{144}Nd_{Chondrite})/^{143}Nd/^{144}Nd_{Chondrite}$. The chondritic value used is $^{143}Nd/^{144}Nd_{Chondrite} = 0.512638$. The data are compiled from the PETDB database (http://petdb.ldeo.columbia.edu). (b) $^{87}Sr/^{86}Sr$ versus ε(Nd) for MORBs compared with data for turbidites and other marine sediments (Ben Othman *et al.*, 1989; Hemming and McLennan, 2001). This illustrates the complementary nature of continent-derived sediments and MORB expected from the relationships shown in Figure 3.

Treatise on Geochem.

Transformations

Métasomatisme (changement de composition du a l'ouverture du système chimique)

- Passage de magmas / fluides
- Reconnaissance → implications

Métamorphisme (transformation à l'état solide, nouvelle minéralogie, nouvelle structure)

- Change P
- Add water BT → Br, Chl, Tr, Serp
- Add water HT → Amph, Chl → fusion ?

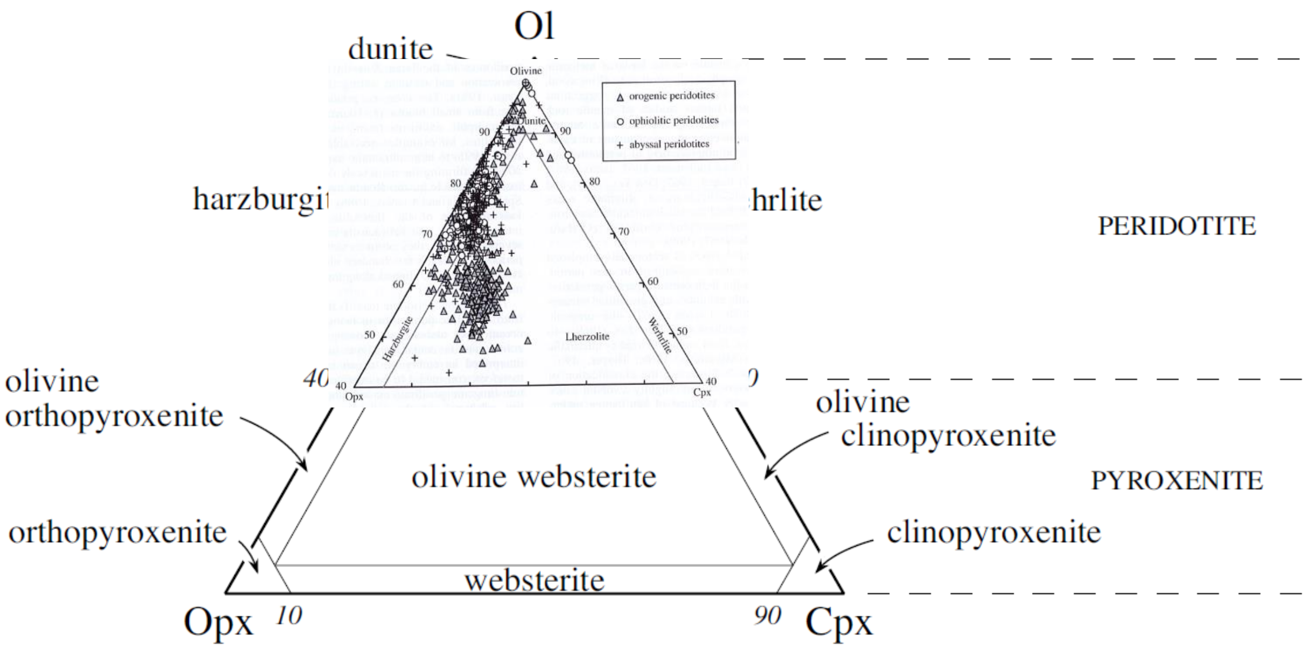

Amphibole
Phlogopite
Carbonates
+- Pyroxenes
+- Ph. Alum
+- Olivine
+- ………

Métasomatisme

Minéralogique
Compositionnelle
Cryptique

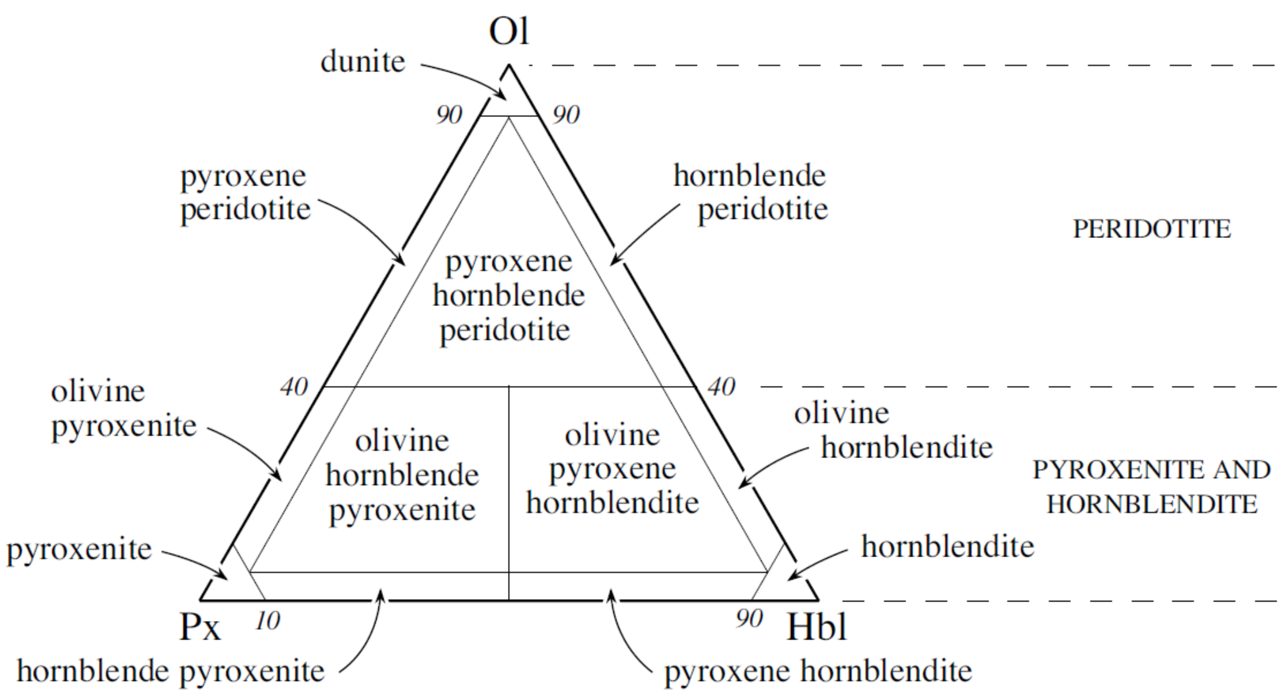

→ Notion de manteau à relativiser
→ Résidu / percolation de magma / « slab remnants… »

Almklovladen Norway

Almklovladen, Norway

Kohistan, Pakistan

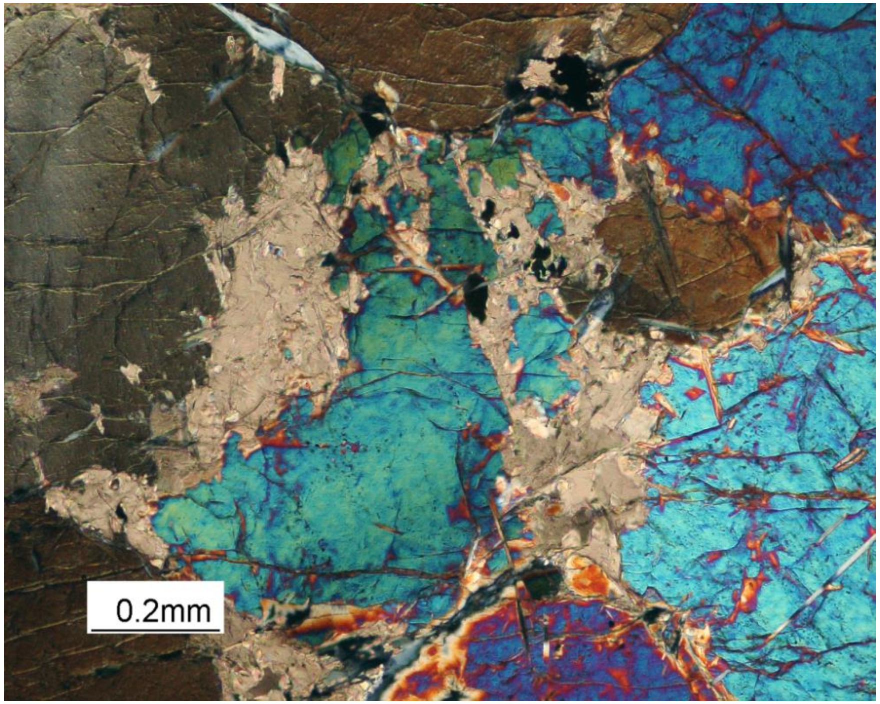
0.2mm

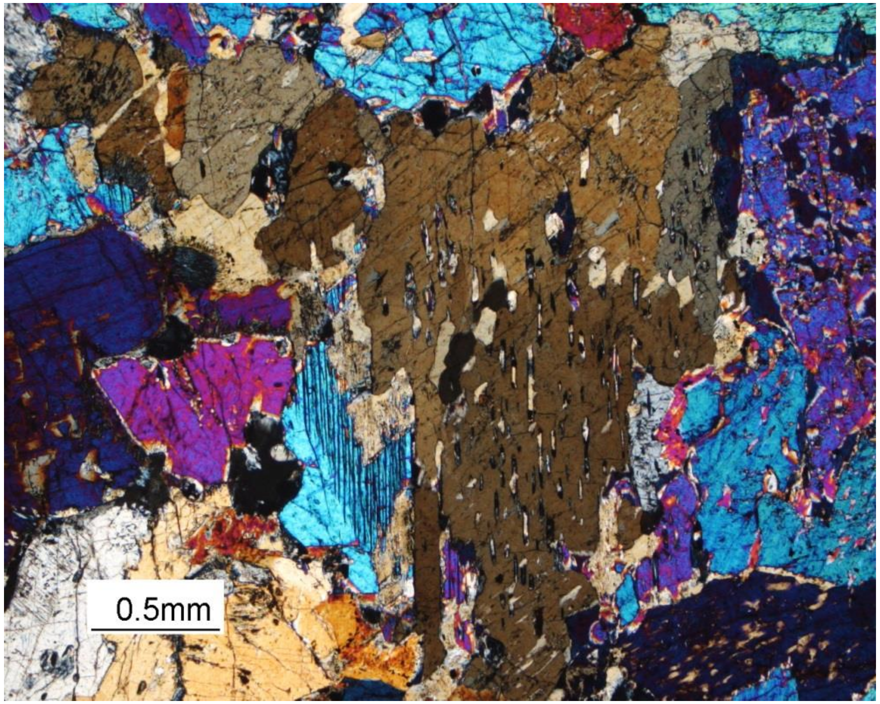
0.5mm

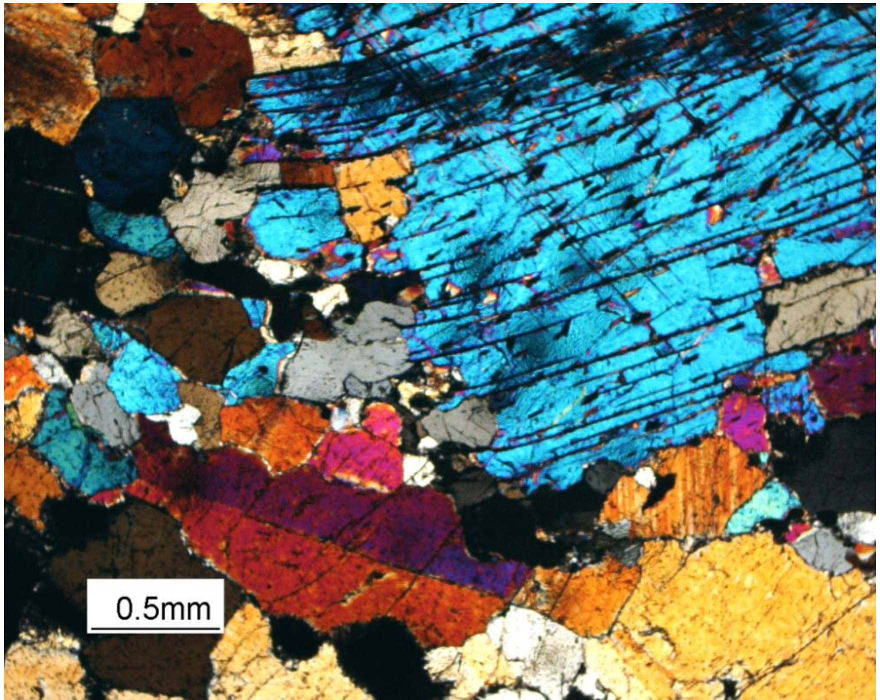
0.5mm

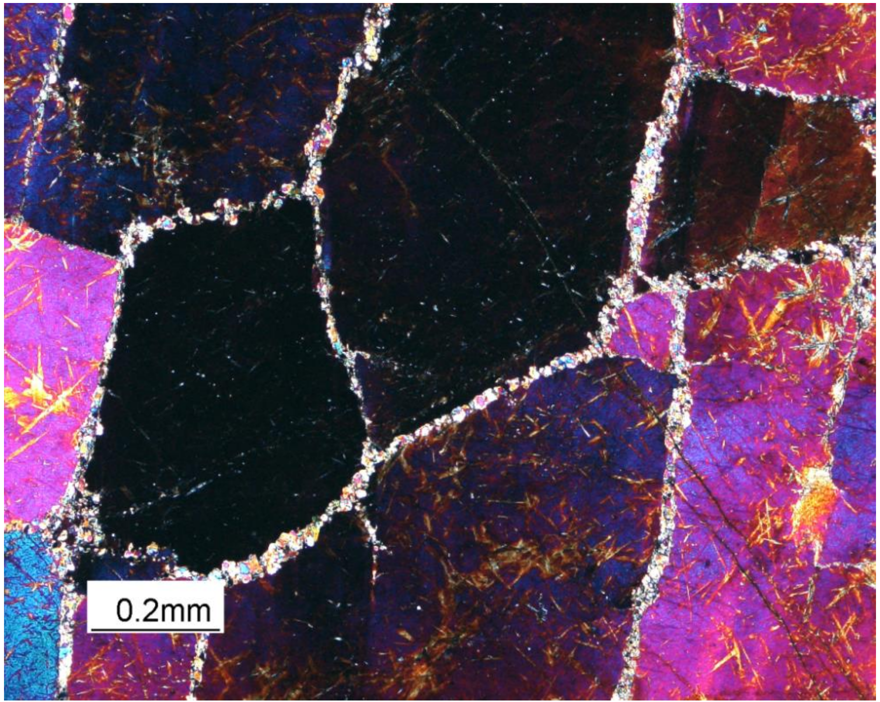
0.2mm

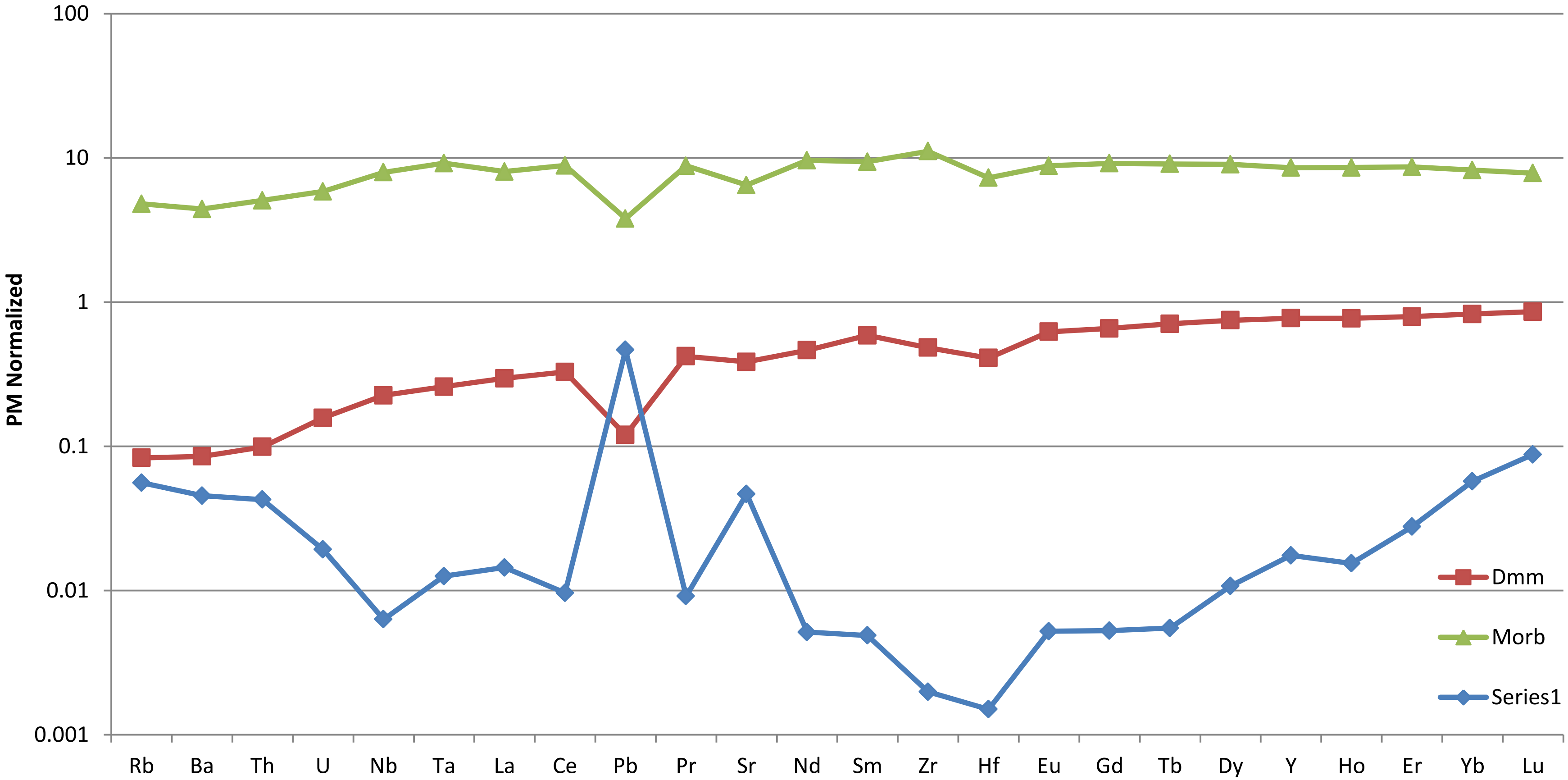

Fusion → Basaltes → Manteau « déplété »

Evènement métasomatique : enrichissement

Métamorphisme (isochimique)

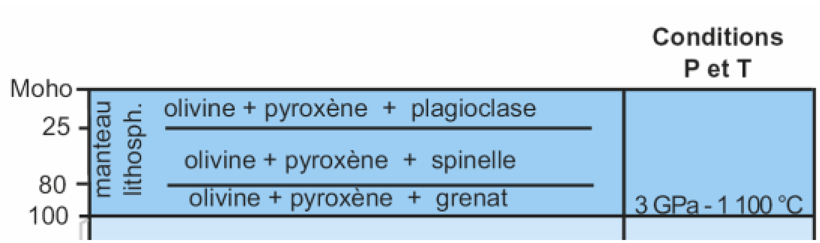

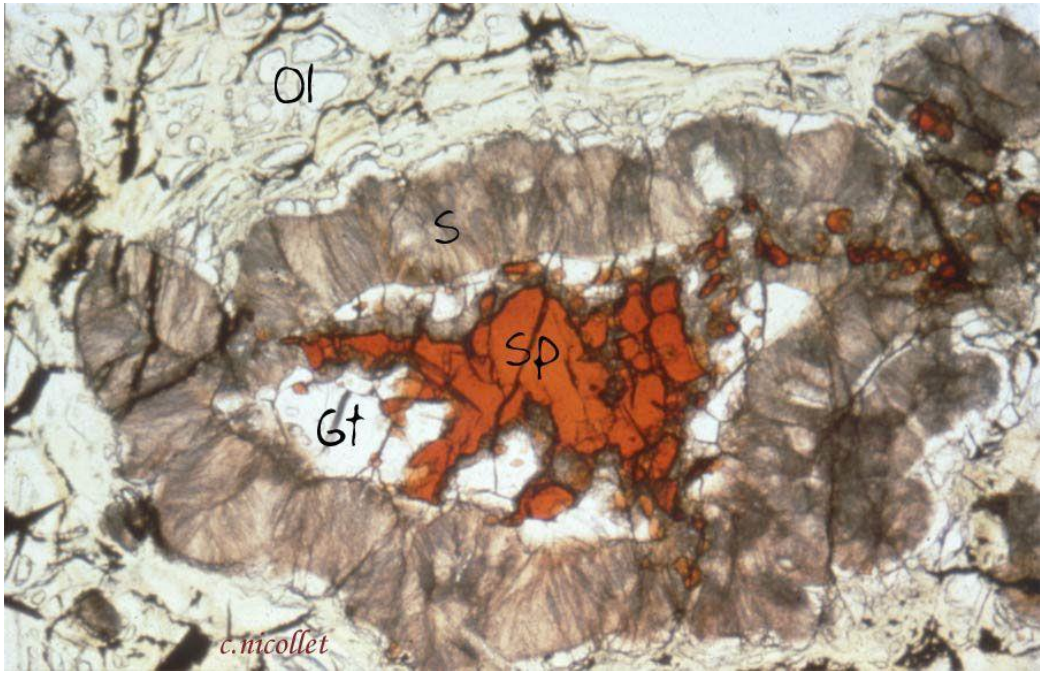

Transition Grt → Sp → plag

(Rare !!)

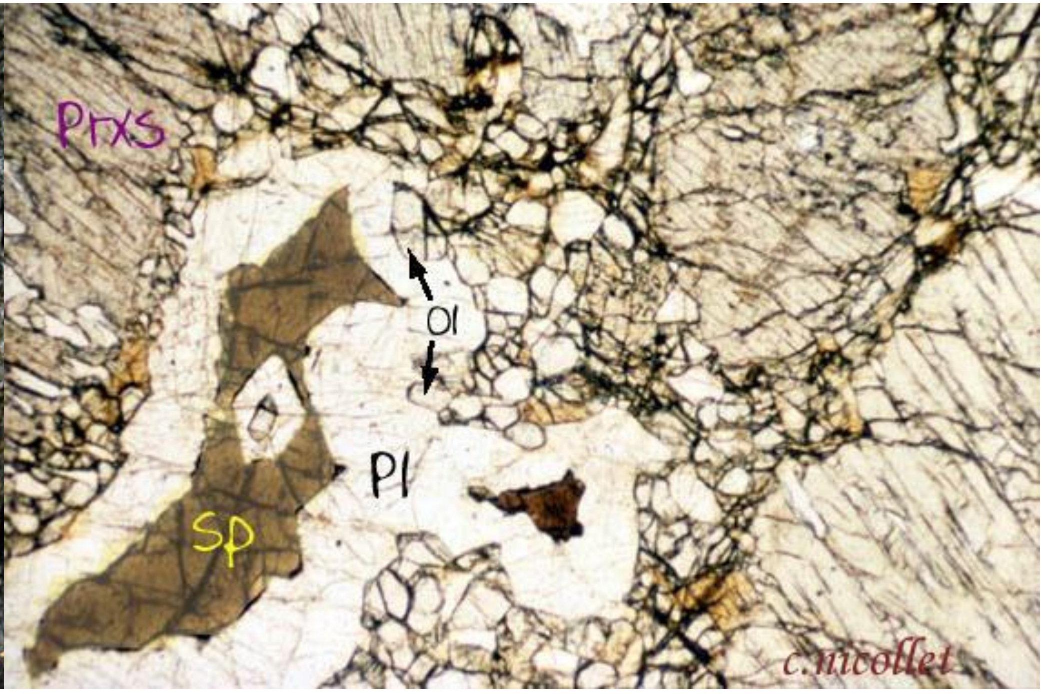

Métamorphisme (non-isochimique)

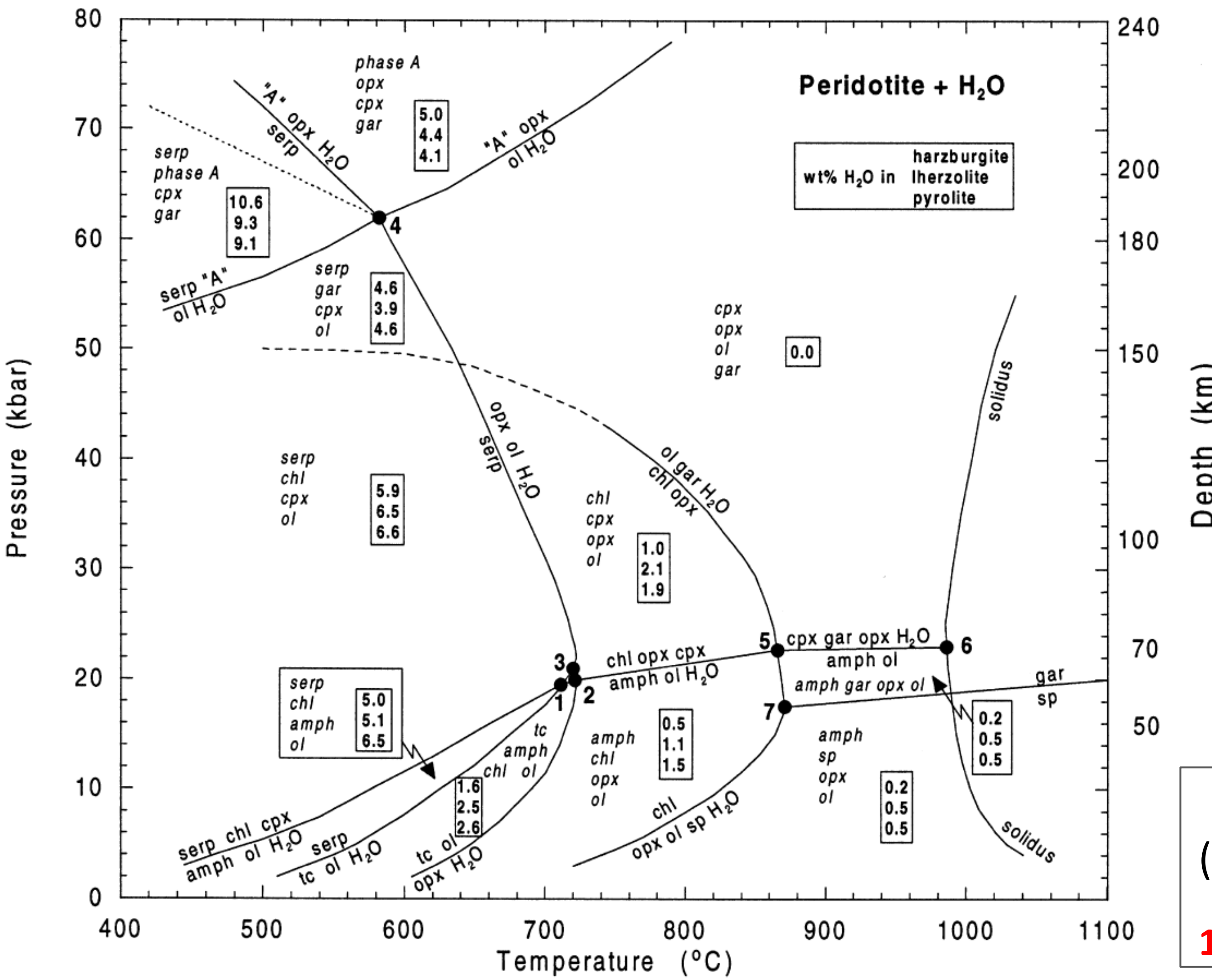

Fig. 5. Phase diagram for H_2O-saturated average mantle peridotite and maximum H_2O contents bound in hydrous phases in average peridotites. Upper value: harzburgite; middle value: lherzolite; lower value: pyrolite. The *italic* labels are assemblages in a given stability field. 'A' = phase A, *amph* = amphibole, *chl* = chlorite, *cpx* = clinopyroxene, *gar* = garnet, *ol* = olivine, *opx* = orthopyroxene, *serp* = serpentine, *sp* = spinel, *tc* = talc.

Serpentine
Chrysotile
Lizardite
Antigorite
$(Mg,Fe)_3Si_2O_5(OH)_4$
12 Wt % H2O

Tremolite
$Ca_2Mg_5Si_8O_{22}(OH)_2$
2 Wt % H2O

Talc
$Mg_3Si_4O_{10}(OH)_2$
4-5 Wt% H2O

Chlorite
$(Mg,Fe)_5Si_3Al_2O_5(OH)_8$
12 Wt % H2O

Schmidt & Poli 98

Transformations roche à la ride (Serp = croute)
Minéralisations !! → Metallogénie
Important pour les zones de subduction …

→ Berceau de la vie ?

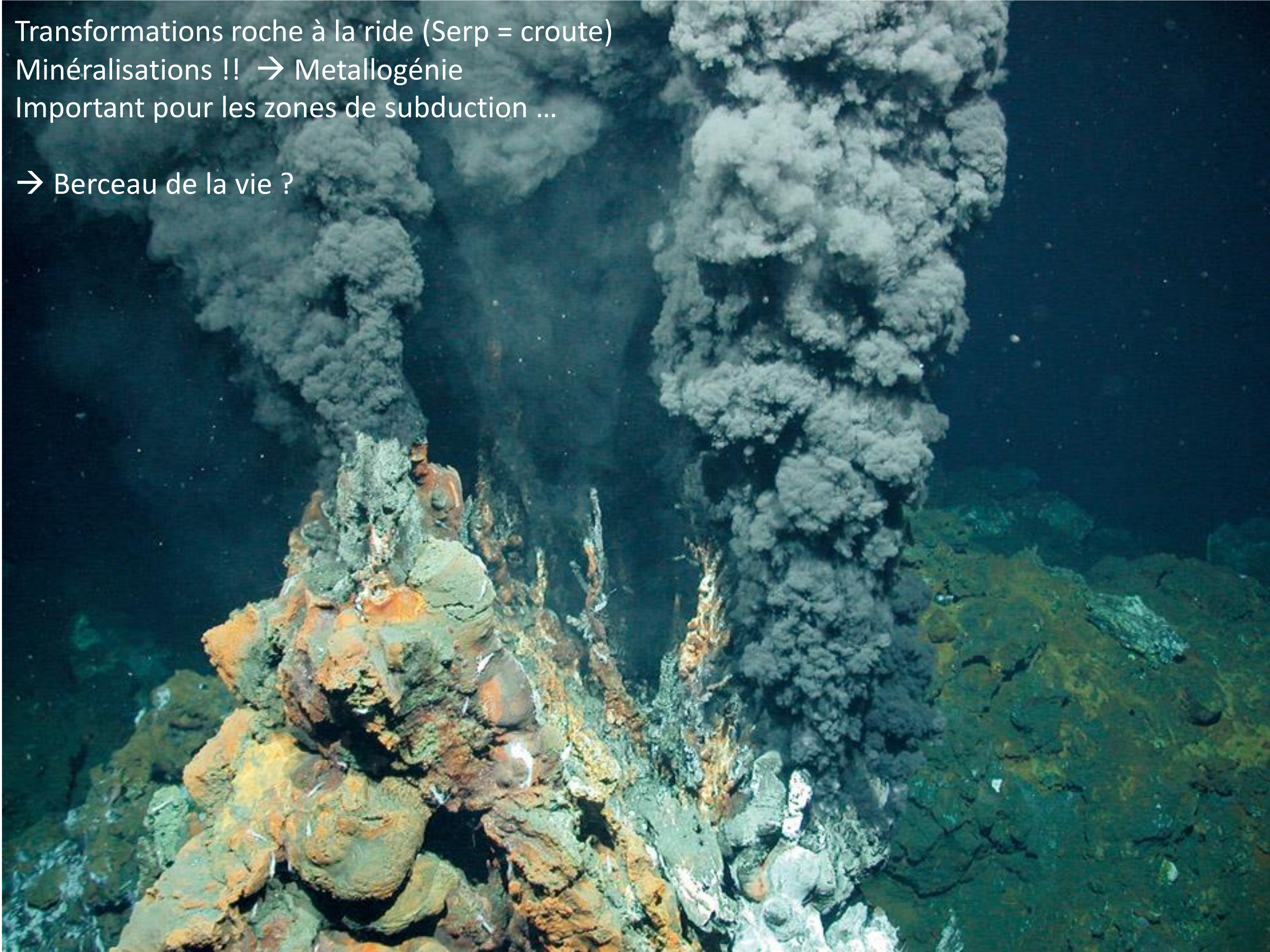

	Roche du manteau			
	Lhz	***Hz***	***Dun***	
SiO2	42.3	39.9	38.3	
Al2O3	4.2	2.3	1.4	
FeO	9.8	11.4	12.6	
MgO	31.2	33.2	37.9	
CaO	5	2.9	1	
Na2O	0.5	0.3	0.2	
K2O	<0.1	<0.1	<0.1	
Cr2O3	0.2	0.3	0.4	
TiO2	0.6	0.3	0.1	

Serpentinite / Alpes

région	**Chenaillet**	**Chenaillet**	**Chenaillet**
échantillons	CH13 /EU	CH14 /EU	CH15 /EU
	P1	P1	P1
SiO2	**39.6**	**39.5**	**39.4**
TiO2	**0.1**	**0.1**	**0.1**
Al2O3	**2.6**	**2.3**	**2.4**
Fe2O3	**8.4**	**8.0**	**8.2**
MnO	**0.1**	**0.1**	**0.1**
MgO	**36.0**	**36.3**	**36.5**
CaO	**0.6**	**0.6**	**0.5**
Na2O	**traces**	**traces**	**traces**
K2O	**traces**	**traces**	**0.02**
P2O5	**0.0**	**0.1**	**0.1**
LOI (H2O)	**13.0**	**13.4**	**13.0**
Total	**100.3**	**100.2**	**100.2**